In situ adenovirus vaccination engages T effector cells against cancer

Sebastian Tuve [a], Ying Liu [a], Khajornsak Tragoolpua [c,d], Jeffrey Daniel Jacobs [a], Roma Christine Yumul [a], Zong-Yi Li [a], Robert Strauss [a], Karl-Erik Hellström [b], Mary Lenora Disis [b,c], Steve Roffler [d,e], André Lieber [a,b,*]

[a] *Division of Medical Genetics, Department of Medicine, University of Washington, Seattle, WA, USA*
[b] *Department of Pathology, University of Washington, Seattle, WA, USA*
[c] *Tumor Vaccine Group, Center for Translational Medicine, University of Washington, Seattle, WA, USA*
[d] *Division of Clinical Microbiology, Department of Medical Technology, Faculty of Associated Medical Sciences, Chiang Mai University, Chiang Mai, Thailand*
[e] *Institute of Biomedical Sciences, Academia Sinica, Taipei, Taiwan*

ARTICLE INFO

ABSTRACT

The efficacy of cancer immunotherapy is limited because of central and peripheral immune tolerance towards tumor-antigens. We propose a novel approach based on the fact that the immune system has not evolved tolerance towards adenoviruses (Ads) and that Ads have not evolved efficient mechanisms for immune-escape. The host-response to intratumoral Ad-vector injection in mice that were immunologically tolerant to *neu*-positive syngeneic mammary-cancer (MMC) was investigated. Intratumoral injection with replication-deficient, transgene-devoid Ad induced immune responses at two different anatomical sites: the tumor-draining lymph nodes and the tumor microenvironment. The lymph nodes supported the generation of both *neu*- and Ad-specific T effector cells, while inside the tumor microenvironment only Ad-specific T cells expanded. Importantly, Ad-specific T cells were anti-tumor-reactive despite the presence of active regulatory T cell-mediated immune tolerance inside MMC tumors and anti-tumor efficacy of Ad was increased by pre-immunization against Ad despite the production of Ad-neutralizing antibodies.

© 2009 Elsevier Ltd. All rights reserved.

1. Introduction

Adenovirus (Ad) serotype 5 based vectors have been developed as therapeutics for cancer in the recent decade and are the most frequently used viral gene vectors in clinical trials [1]. Ads have naturally evolved to efficiently infect a wide variety of cells, rapidly complete their life cycle (viral genome replication, viral protein expression, progeny viral particle assembly) and lyse the host cell within this process. Accordingly, one therapeutic strategy has been to restrict Ad-replication to tumor cells ("oncolysis") [2]. As a different approach, injection with E1-deleted, replication-deficient Ads has been used to express various therapeutic transgenes in tumors.

In clinical trials Ad-vectors have been generally safe. When systemically applied, Ad-vectors have not had significant anti-tumor efficacy. This has been, in part, attributed to cellular and non-cellular blood components that efficiently bind Ads and sequester it in particular to the liver and spleen upon application into the blood stream [3,4]. In contrast, when Ads are directly injected into

tumors, efficacy has been observed in multiple clinical phase I–III trials [5–8]. One of the most frequently used Ad-vectors worldwide is ONYX-015 a.k.a. H101, which is oncolytic [5–8]. Another Ad.IR-based oncolytic Ad-vector (which has been developed in our laboratory) strictly expresses its transgenes upon replication of the Ad genome as a result of homologous recombination between inverted repeats (IR), which occurs in cancer cells but not in non-malignant cells ([9,10] and Fig. S1).

In this study we investigated the role of immune responses to intratumorally delivered Ad-vectors. We hypothesized that the immune system could either enhance or decrease the efficacy of Ad-vectors that are directly applied into the tumor.

The immune system could decrease the efficacy of Ad-vector therapy since it has evolved to efficiently and rapidly recognize Ads as pathogens in an innate and adaptive manner [11]. This combined innate and adaptive response upon natural Ad-infection most commonly results in Ad-clearance and life-long immunity in the majority of hosts [11]. The innate recognition process is initiated by Ad DNA/capsid sensors (which include toll like receptor 9 (TLR9) and the inflammosome) and peaks within the first min/h of Ad-infection [12–14]. The subsequent adaptive response is thought to require the integration of both Ad-specific $CD4^+$ and $CD8^+$ T cell responses. Ad-specific cytotoxic T lymphocytes (CTLs) are preferen-

---

tially directed towards conserved Ad-epitopes within the Ad-capsid (mostly Ad-hexon protein) and kill infected cells (using multiple mechanisms that include perforin, Fas-L and TNFα), which disrupt the Ad life cycle before progeny viruses are assembled. Ad-specific antibodies are frequently targeted against the serotype-specific ("hypervariable") Ad-epitopes that are located on the surface of the viral particle and circulate through the periphery to functionally neutralize Ads [15,16].

In contrast to an inhibitory function, Ad-triggered immune responses could also synergize with anti-tumor effects, e.g. because replication of the virus could be involved in releasing tumor-specific antigens to dendritic cells and innate and adaptive immune responses triggered by adenoviruses could create a pro-inflammatory environment inside the tumor that could facilitate the activation of tumor-antigen-specific T cells, thereby triggering not only anti-virus but also anti-tumor immunity. This hypothesis is under investigation for a variety of viral vectors, including adenovirus vectors, and being tested in pre-clinical models and clinical trials [17,18].

To investigate immunological responses to Ad-vector-mediated cancer therapy one needs an immunocompetent syngeneic model that allows Ad-infection and Ad-replication. Since human Ads rarely replicate in non-human cells few such models are available, including Syrian hamsters, cotton rats, mice and canines [19–22] and it was not investigated in any of these models whether the Ad-induced immune response itself could have a function in anti-tumor efficacy.

This is the first study to systematically investigate immune responses towards both Ad-vector- and tumor-antigens in immunocompetent animals. Towards this goal we characterized a novel syngeneic *in vivo* model. We found that mouse mammary carcinomas (MMC) in *neu*-transgenic mice supported Ad-infection and Ad-replication *in vivo*. Similar to human breast cancers, MMC tumors induced *neu*-specific T effector cells in the sentinel lymph nodes (LN). Surprisingly, we found that the dominant anti-tumor mechanism of intratumoral Ad-vector injection was the induction of Ad-specific, and not *neu*-specific, T effector responses.

2. Materials and methods

2.1. Mice and cells

Neu-transgenic (*neu-tg*) *mice* [strain name: FVB/N-Tg(MMTVneu)202Mul] were obtained from the Jackson Laboratory (Bar Harbor, ME). These mice harbor non-mutated, non-activated rat *neu* under control of the mouse mammary tumor virus (MMTV) promoter. The *neu* transgene is expressed at low levels in normal mammary epithelium, salivary gland, and lung. Until the age of 8 month ~35% of female *neu*-tg mice spontaneously develop mammary carcinomas that display high *neu*-expression levels. CTLs specific for the immunodominant H-2Dq/RNEU$_{420-429}$ epitope can be detected in *neu*-tg mice using the corresponding tetramer [23]. *Mouse mammary carcinoma* (*MMC*) *cells* were established from a spontaneous tumor in a *neu*-tg mouse. MMC cells have been shown to display high levels of *neu*-expression, an epithelial phenotype, expression of MHC class I and II and presentation of the immunodominant *neu*-epitope H-2Dq/RNEU$_{420-429}$ [24]. Culture conditions for MMC cells were RPMI-1640 medium containing 10% fetal bovine serum (FBS), 2 mM L-glutamine (Gln), 100 U/ml penicillin (P), and 100 μg/ml streptomycin (S). *Immunodeficient* (*SCID*) *mice* [strain name: NOD.CB17-Prkdc^{scid}/J] were obtained from the Jackson Laboratory. These mice are homozygous for the severe combined immune deficiency spontaneous mutation (Prkdc^{scid} a.k.a. SCID), which is mainly characterized by an absence of functional T cells and B cells, lymphopenia, hypogammaglobulinemia, and a normal hematopoietic microenvironment. *Human*

cancer cell lines: Human lung epithelial cancer cells (A549) and human embryonic kidney derived cells (293) were both obtained from the ATCC (Manassas, Virginia) and cultured in Dulbecco's modified eagle medium (DMEM) supplemented with 10% FBS, Gln/P/S. 293 cells express the human Ad5-E1 genes and were used for propagation of E1-deleted Ad-vectors and pfu-assays (see below).

2.1.1. Adenovirus vectors

All vectors were based on Ad serotype 5 and had the E1A and E1B genes (nucleotides 342–3523) and the E3 genes (nucleotides 28,133–30,818) deleted (with the exception of H101; see below). The structure of all vectors is shown in Suppl. Fig. 2. Ad.zero is a control vector that lacks a transgene. Ad.GFP and Ad.lacZ are vectors that express the corresponding reporter genes. Ad.IR-GFP and Ad.IR-lacZ express the reporter genes in a replication-dependent manner. Ad.αCD3 and Ad.αCD137 express membrane bound forms of mouse monoclonal antiCD3 and antiCD137 scFv, respectively. Ad.IL-15 and Ad.LIGHT express the secreted mouse cytokines IL-15 and LIGHT, respectively. Ad.IR-E1A/AP expresses the adenoviral E1A protein and human alkaline phosphatase in a replication-dependent manner. Ad.IR-E1A/TRAIL expresses the adenoviral E1A protein and human TRAIL in a replication-dependent manner.

Recombinant viruses were propagated in 293 cells, banded in CsCl gradients, dialyzed and stored in aliquots as described [25]. To assess contamination of AdE1$^-$ vector preparations with E1$^+$ replication-competent adenovirus (RCA), real-time PCR quantification for AdE1$^+$ genomes was performed [10]. Only virus preparations that contained less than one E1$^+$ (RCA) viral genome in 1×10^9 genomes were used. Ad-particle (viral particle, VP) concentrations were determined spectrophotometrically by measuring the optical density at 260 nm (OD$_{260}$). Plaque titering (plaque forming units, pfu) was performed using 293 cells as described elsewhere [25]. The pfu:VP ratios for all Ad preps were ~1:20. Multiplicities of infection (MOIs) in this study were stated as pfu per cell (pfu/cell) for all assays. Endotoxin contamination was tested with an Endotoxin detection kit (BioWhittaker, Walkerville, MD). All vectors were free of endotoxin.

2.1.2. Real-time PCR

Real-time PCR was performed using a LightCycler (Roche) and the QuantiTect^{TM} Sybr® Green PCR Kit (Qiagen). For transcript analysis total RNA from samples was extracted using the RNeasy Mini Kit (Qiagen). RNA was reverse transcribed and genomic DNA was removed using the QuantiTect Reverse Transcription Kit (Qiagen). For DNA analysis total DNA from samples was extracted and RNA removed using the Blood and Cell Culture DNA Mini Kit (Qiagen). Conditions for real-time PCR were 15 min at 95 °C followed by 50 amplification cycles (20 s at 60 °C, 20 s at 72 °C and 15 s at 95 °C). Primer pairs for amplification are listed in Tab. S1. Specificity of amplification products was confirmed using melting curve analysis and agarose gel electrophoresis. Positive samples were used to generate standard curves. Transcript/DNA levels were presented as fold increase. Transcript/DNA input was normalized using β-actin control primer.

2.1.3. Flow cytometry

Flow cytometry was performed using a BD FACSCalibur (BD Biosciences, San Diego, CA). Samples were pre-treated with Fc-block (anti-CD16/CD32, BD Biosciences) for 15 min, stained for 30 min on ice in washing buffer (WB; PBS-1%FBS) and washed three times with WB. FITC- or PE-conjugated isotype-controls were included in all experiments. Anti-E-cadherin-PE antibody (clone 114420, R&D Systems, Minneapolis, MN) was used to detect MMC cells. For flow-cytometry analysis of immune cells the following monoclonal

antibodies (mAbs) were used: anti-FoxP3-PE (clone FHK16s; cells were permeabilized according to the manufacturer's instruction; eBioscience), anti-CD4-FITC (clone RM4-5), anti-CD8-FITC (clone 53-6.7), anti-NK1.1-PE (clone PK136), anti-CD80 (clone 16-10A1), anti-CD86 (clone GL1) (all from BD Biosciences). The PE-labeled H-2Dq/RNEU$_{420-429}$ (H-2D(q)PDSLRDLSVF) tetramer was obtained from the National Institute of Allergy and Infectious Diseases MHC Tetramer Core Facility (Atlanta, GA) and used according to the manufacturer's instructions.

2.1.4. Lymphocyte enrichment

In order to enrich specifically for lymphocytes, samples (spleens, inguinal lymph nodes, tumors) were minced and filtered through a 70-μm cell strainer (BD Biosciences). Spleen suspensions were additionally treated with BD PharmLyse (1:10 dilution; BD Biosciences) for 1 min at RT and washed twice in WB. Tumor-infiltrating lymphocytes (TIL) were separated from tumor cells and erythrocytes by centrifugation of the tumor cell suspension on a Ficoll gradient (Histoplaque 1083, Sigma). For this cell suspensions were layered onto the top of the gradient in a 15-ml Falcon tube followed by centrifugation at $800 \times g$ for 50 min at RT without braking. Lymphocytes were collected and washed twice in WB.

2.1.5. Isolation of intratumoral cells

To generate viable single-cell suspensions of MMC tumors that contained all intratumoral cell fractions (in particular MMC, immune and stroma cells) for flow-cytometry analysis, tumors were minced into small pieces and then immersed in 5 ml digestion mixture (RPMI-1640 with 10% fetal bovine serum, 50 μl of 1% collagenase, and 50 μl of 1% DNase (both from Life Technologies, Carlsbad, CA)). This mixture was incubated in a water bath at 37 °C for 2 h and mixed by pipetting every 20 min. 5 ml Versene (Gibco) was then added and the mixture was incubated in a water bath at 37 °C for another 1 h, mixed by pipetting every 20 min, and then filtered through a 70-μm screen followed by washing twice in WB.

2.1.6. ELISpot

For quantification of Ad-specific T cells, splenocytes of naïve neu-tg mice were ex vivo pulsed with Ad.zero (MOI 50 pfu/cell) as described before [26]. Lymphocytes from spleen, LN, and tumor were harvested and 1×10^6 cells (spleen, LN) or 2.5×10^5 cells (TIL) were mixed with 1×10^6 ex vivo pulsed splenocytes for in vitro sensitization. After 24 h of incubation in 96-well plates, cells were plated in anti-IFN-γ-coated wells of ELISpot plates (Millipore, Bedford, MA). 24 h later, plates were washed and the spots of IFN-γ-producing T cells were counted.

2.1.7. Immunohistochemistry/immunohistofluorescence

MMC cells were cultured in Lab-Tek 8-well chamber glass slides (Nalge Nunc International, Rochester, NY). MMC tumors were cryofixed in OCT compound (Miles, Elkhart, Ind.) and Cryomolds (Tissue-Tek, Torrance, CA), cut with a cryostat in 8 μm sections that were transferred to glass slides. LacZ: For detection of lacZ expression slides were fixed with a solution containing PBS, 0.5% glutaraldehyde, and 1 mM MgCl$_2$ (0.5% glutaraldehyde-PBS) for 20 min at room temperature (RT) and incubated with 5-bromo-4-chloro-3-indolyl-β-D-galactopyranoside (X-Gal). Reaction was stopped by washing with PBS. Slides were mounted with Vecta Mount Medium (Vector Laboratories, Burlingame, CA). AP: For detection of AP expression, slides were fixed using 0.5% glutaraldehyde-PBS for 30 min at RT. After the samples were washed with PBS, they were incubated at 65 °C for 1 h to inactivate endogenous AP. Staining was performed in a solution containing 0.1 M Tris (pH 9.5), 0.1 M NaCl, 0.5 mg of NBT (4-nitroblue tetrazolium chloride) (Roche Diagnostics) per millilitre, and 0.1875 mg of BCIP (5-bromo-4-chloro-3-indolylphosphate) (Roche Diagnostics)

per millilitre. Reaction was stopped by washing with PBS. Slides were mounted with Vecta Mount Medium (Vector Laboratories). Antibodies: Slides were fixed with acetone/methanol (10 min) and washed twice with PBS. Slides were blocked for 20 min at RT using PBS-5% blotting grade milk (BIO-RAD, Hercules, CA) followed by incubation with primary antibodies in PBS for 1 h at RT. Then slides were washed twice with PBS and incubated with secondary antibodies for 1 h at RT followed by washing with PBS three times. Slides were washed twice with PBS, mounted with Mounting Medium for Fluorescence (Vector Laboratories) and then analyzed using a fluorescence microscope. Laminin was detected using anti-laminin polyclonal (primary) antibody (1:200; #Z0097; Dako, Carpinteria, CA) and goat anti-rabbit-IgG AlexaFluor568 (secondary) antibody (1:200; Molecular Probes, Carlsbad, CA); Hexon was detected using FITC-conjugated goat-anti human Ad-hexon antibody (1:100; cat. no.: AB1056F; Chemicon International) or Cy3-labeled mouse anti-human Ad-hexon antibody (1:100; clone 20/11; Chemicon International); Cell surface markers: FITC-labeled anti-E-cadherin antibody (1:100; clone 36/E-Cadherin, BD Biosciences) or FITC-labeled anti-CD4/CD8/NK1.1 antibodies (see flow cytometry). Nuclei were stained with 4′,6-diamidino-2-phenylindole (DAPI; Sigma). Apoptosis: TUNEL assay was performed using ApopTag® Peroxidase In Situ Apoptosis Detection Kit (Chemicon International, Millipore Corporation, Billerica, MA) according to the manufacturer's instructions, except for the usage of anti-Digoxigenin-Rhodamine (1:60; Boehringer Mannheim, Ingelheim, Germany) instead of anti-Digoxigenin-Peroxidase. TUNEL positive cells were detected and counted using a fluorescence microscope (40× Magnification; 20 random viewing fields per section; 10 sections per tumor).

2.1.8. Cytotoxicity assays

Cells that were incubated with Ad-vectors and/or lymphocytes were continuously monitored for signs of cytotoxicity. Cytotoxicity was defined as the presence of both a discontinuous cellular monolayer ("gaps") and detached ("round") cells at the same time. For crystal violet staining cells were washed with PBS and fixed with 4% paraformaldehyde for 5 min at RT. Fixed cells were washed with PBS and incubated for 3 min in 1% crystal violet in 70% ethanol, followed by three rinses with water. Air-dried cells were photographed.

2.1.9. Ad-neutralizing antibodies

100 μl of blood was extracted from immunized and non-immunized mice using retro-orbital eye bleeding followed by centrifugation of samples at room temperature and collection of the supernatant. Serum samples were stored at −80 °C. For determining the titer of neutralizing antibodies, serial (1:2) serum dilutions were generated for each sample, Ad5 weight was added for 1 h at RT to each dilution and samples were applied to 293 cells, which were monitored for CPE for 7 days.

2.1.10. Animal experiments

Neu-tg and SCID mice were bred under specific pathogen-free conditions at the University of Washington (Seattle, WA). Animal care and use was in accordance with institutional guidelines. Female mice at the age of 6–10 weeks were used for all experiments. Tumor cell transplantation: MMC cells were harvested using Versene (Gibco) and washed in RPMI-1640 medium (without supplements) before injection. Mice received anesthesia (Avertin i.p.) and were injected with 5×10^5 MMC cells (diluted in 100 μl RPMI-1640 without supplements) subcutaneously on the right mid-dorsum with a 23-gauge needle. Tumors were measured every other day and tumor volume was calculated as the product of length × width × width. For survival studies tumor sizes ≥500 mm^3 were considered the experimental endpoint. Animals with tumor sizes ≥500 mm^3 received anesthesia (Avertin i.p.) and were sacrificed via cervical neck dissection. Animals with skin surface

ulcerations were excluded from experiments and sacrificed immediately. *Intratumoral Ad-injection:* When MMC tumors reached a size of 3–4 mm diameter, mice were randomly assigned to treatment groups. Mice were given anesthesia (Avertin i.p.) and then Ad (1×10^9 pfu diluted in 50 μl PBS) or 50 μl PBS was intratumorally injected with constant and low pressure using an insulin syringe (BD Pharmingen). *Antibody-mediated lymphocyte depletion.* CD4+/CD8+ T cells and NK cells were depleted using i.p. injection of the following antibodies diluted in 500 μl PBS: 200 μg rat anti-mouse CD4 IgG (GK1.5, ATTC), 200 μg rat anti-mouse CD8 IgG (169.4; ATTC) or 20 μl rabbit anti-mouse asalio GM1 IgG (Cedarlane, Ontario, Canada). 200 μg of the respective IgG isotype-control (Jackson ImmunoResearch, West Grove, PA) was used in control animals (isotype1, rat IgG; isotype2, rabbit IgG). For some experiments injection of each antibody was repeated every 3 days to maintain the depletion. Anti-mouse CD4 and anti-mouse CD8 antibodies were produced in SCID mice, purified from ascites using standard protein G column purification, dialyzed against PBS and stored at −80 °C. Depletion efficacy of antibodies was tested in *neu*-tg mice (Fig. S10). *Ad-immunization*: For establishing pre-existing anti-Ad immunity 2.5×10^9 pfu Ad.zero was injected intramuscularly (in 100 μl PBS) or intraperitoneal (in 500 μl PBS). A second injection was performed 14 days later using 1×10^9 pfu.

2.1.11. Statistical analysis

Statistical significance of *in vivo* data was analyzed by Kaplan–Meier survival curves and logrank test (GraphPad Prism Version 4). Statistical significance of *in vitro* data was calculated by two-sided Student's *t*-test (Microsoft Excel). *P* values >0.05 were considered not statistically significant (n.s.). *P* values <0.05 were considered statistically significant (*$P < 0.05$; **$P < 0.01$; ***$P < 0.001$).

3. Results

3.1. Ad-vectors

In this study the following 12 vectors divided into four categories were tested (see Section 2 and Fig. S2): (A) *Control vector* (Ad.zero): an E1/E3-deleted, replication-deficient vector that was devoid of transgenes. (B) *Reporter-gene expressing vectors*: Expressing reporter genes independent of viral replication (Ad.GFP, Ad.lacZ) or strictly upon viral replication (Ad.IR-GFP, Ad.IR-lacZ; see Figs. S1, S2 and refs. [9,10]). (C) *Immunoadjuvant-expressing vectors*: Towards the goal of increasing an anti-tumor immune response we constructed Ad-vectors expressing the following well characterized immunoadjuvants that have previously shown to trigger NK- and/or T cell-mediated anti-tumor immune responses: anti-CD3scFv (triggers CD3 signaling [27,28]), anti-CD137scFv (triggers signaling via the CD137 co-stimulatory molecule [29,30]), IL-15 (activates T effector but not regulatory T cells via IL-15R receptor [31]) and LIGHT (activates T and NK cells via multiple receptors [32]). (D) *Oncolytic vectors*: Towards the goal of increasing anti-tumor efficacy via tumor-specific viral replication the following oncolytic vectors were included: H101 (a.k.a. ONYX-015) has been the most common oncolytic vector in clinical trials [5–8]. Ad.IR-E1A/TRAIL has been developed in our laboratory and shown to express E1A and pro-apoptotic TRAIL in a strictly replication-dependent manner in cancer cells [33].

3.2. Ad-vectors induce replication- and immune-mediated cytotoxicity in MMC cells in vitro

Since mouse cancer cells rarely support both infection and replication of human Ads, we first tested syngeneic mouse cell lines for their susceptibility towards human Ads. For this purpose we utilized Ad-vectors that expressed GFP independent (Ad.GFP) or dependent (Ad.IR-GFP) on viral genome replication [9,10]. Mouse mammary-cancer cells (MMC; derived from syngeneic tumor-antigen *neu*-transgenic mice [23]) supported Ad-mediated GFP expression which was dependent and independent of Ad-vector replication (Fig. 1A). This was confirmed by using hydroxyurea to inhibit adenoviral replication [10] which impaired GFP expression via Ad.IR-GFP but not via Ad.GFP (Fig. 1A). Ad.IR-GFP-mediated GFP expression was more than 100-times less as compared to Ad.GFP-mediated expression of this transgene. This indicated that replication-independent transgene expression was more efficient than replication-dependent transgene expression. We further confirmed that MMC cells supported Ad.IR-mediated expression of other transgenes including lacZ and alkaline phosphatase (AP) using Ad.IR-lacZ and Ad.IR-E1A/AP, respectively (data not shown).

Next we looked for adenoviral proteins that are naturally expressed during adenoviral replication. To do this we chose the Ad-hexon protein since it is an abundant component in the adenoviral capsid and typically over-expressed at a late stage of adenoviral replication. We compared two vectors that were either replication-competent (Ad.IR-E1A/TRAIL) or replication-deficient (Ad.zero). Using immunofluorescence, nuclear expression of Ad-hexon protein was detected only for Ad.IR-E1A/TRAIL-infected but not for Ad.zero-infected MMC cells, indicating that only Ad.IR-E1A/TRAIL vector replicated (Fig. 1B). However, we have previously shown that human cancer cells also support low-level background replication of E1/E3-deleted replication-deficient Ads (although this usually does not induce CPE; [9,10]). Therefore we further investigated Ad.zero and Ad.IR-E1A/TRAIL replication in MMC cells using highly sensitive real-time RT PCR for the detection of E1A (early replication-stage transcript) and hexon mRNA (late replication-stage transcript). Ad.IR-E1A/TRAIL-infected but not (E1/E3-deleted) Ad.zero-infected MMC cells showed E1A transcripts expression (Fig. 1C). However, hexon mRNA was detectable in *both* Ad.zero and Ad.IR-E1A/TRAIL infected cells. Notably, hexon transcript levels in Ad.zero infected MMC cells were more than 100-fold lower. Next, we tested whether MMC cells supported the amplification of viral genomes and the production of progeny infectious viral particles (plaque forming units; pfu), comparing vectors that were either replication-competent (Ad.IR-E1A/TRAIL) or replication-deficient (Ad.zero). For Ad.IR-E1A/TRAIL we detected a ~4-fold increase of genome levels 5 days post infection which indicated genomic replication, although this was less efficient than in human A549 cells, where a ~58-fold increase of genome levels was detected (Fig. 1D, left panel). However, MMC cells apparently did not produce progeny infectious viral particles (compare with human A549 cells as a positive control; Fig. 1D, right panel). In contrast to replication-competent Ad.IR-E1A/TRAIL, for replication-deficient Ad.zero no significant Ad-genome or Ad-pfu production was measurable in both MMC and human A549 cells (Fig. 1D, right panel). Next, the effect of viral replication on CPE formation in MMC cells was tested this time using various Ad-vectors at different MOIs (Figs. 1E, S4). MMC cells supported CPE formation induced by replication-competent vectors (Ad.IR-E1A/TRAIL and H101) at an MOI of ~25 pfu/cell, which was comparable to human A549 cancer cells. In contrast, replication-deficient vectors (Ad.zero, Ad.lacZ) did not induce CPE in MMC or A549 cells (but did in 293 cells that stably expressed human Ad-E1 genes).

Together, the results indicate that MMC cells supported a low-level replication of E1/E3-deleted Ad-vectors, although this did not induce CPE (Figs. 1, S4). Efficient replication and CPE formation in MMC cells was critically dependent on the Ad-E1A gene, since E1A-encoding vectors induced CPE (Ad.IR-E1A/TRAIL, H101) and E1A-deleted vectors did not (Ad.zero, Ad.lacZ; Figs. 1E, S4). These findings are in agreement with our previous studies in human cancer cells [9,10,33].
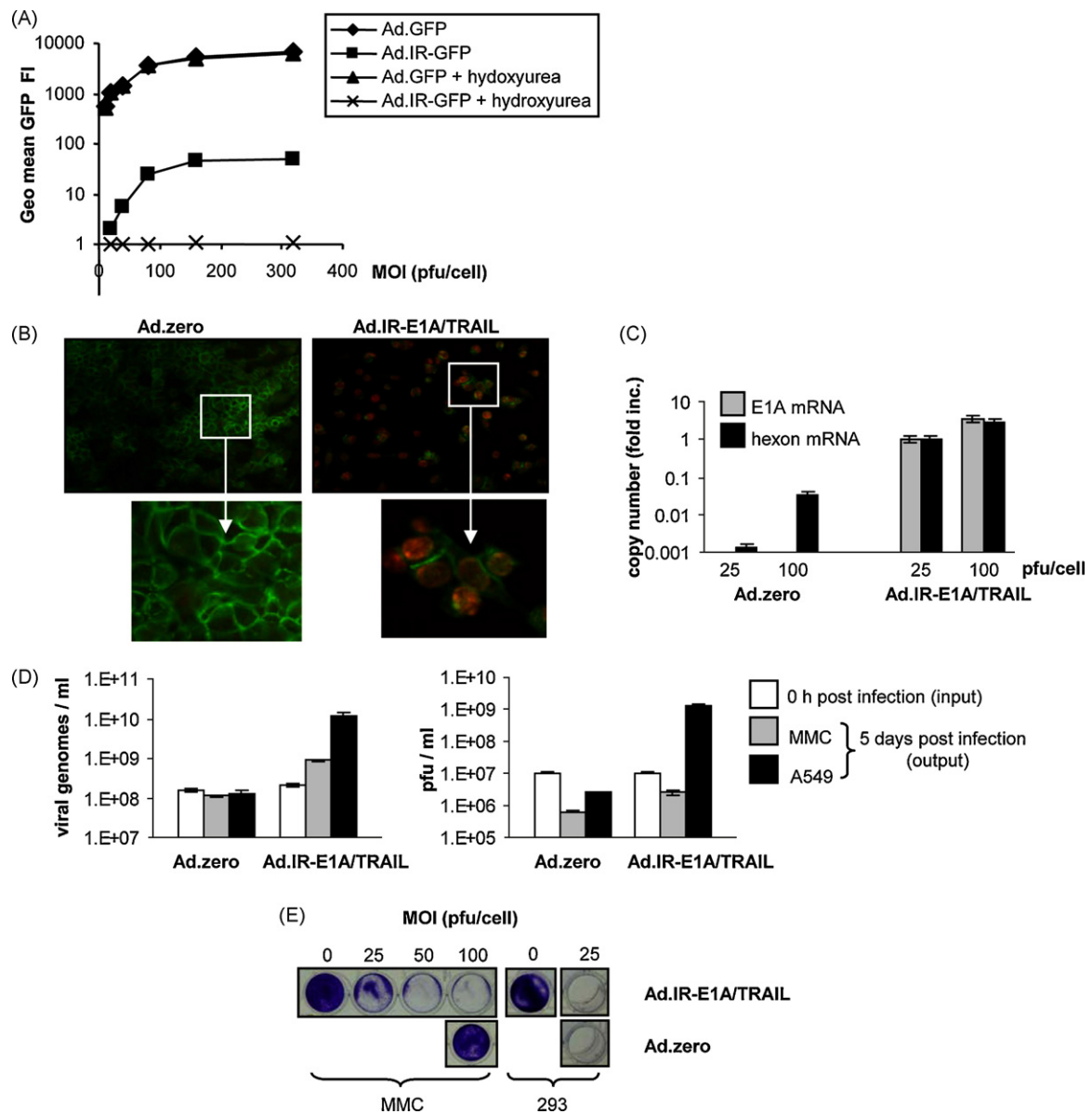
Fig. 1. Ad-replication *in vitro*. (A) GFP detection via flow cytometry in Ad.GFP and Ad.IR-GFP transduced MMC cells (3 days post infection [p.i.]). Hydroxyurea was used to inhibit Ad-replication. (B) Detection of hexon protein in Ad.zero and Ad.IR-E1A/TRAIL transduced cells (3 days p.i.; MOI 100 pfu/cell; positive cells show red nuclear staining; anti-E-cadherin-FITC was used as a cell surface marker). Representative pictures are shown, magnification 20× (upper panel); 40× (lower panel). (C) Relative quantification of E1A and hexon mRNA expression in Ad.zero and Ad.IR-E1A/TRAIL infected MMC cells using real-time RT PCR (7 days p.i.). $y = 1$ for Ad.IR-E1A/TRAIL infected cells (MOI 25 pfu/cell). (D) Absolute quantification of viral genomes and plaque forming units (pfu) in Ad.zero and Ad.IR-E1A/TRAIL infected MMC and A549 cells (0 h and 5 days p.i.). (E) CPE formation in MMC and 293 cells after Ad.zero and Ad.IR-E1A/TRAIL infection (5 days p.i.); (D and E) Bars indicate the mean values and SD of experiments performed in duplicates. (For interpretation of the references to color in this figure legend, the reader is referred to the web version of the article.)

We next tested whether MMC cells supported the Ad-vector mediated expression of the following immunoadjuvants: αCD3scFv, αCD137scFv, LIGHT or IL-15 (Fig. S2). The first two immunoadjuvants are membrane-bound scFvs ([27–30] and Fig. S3). Surface expression of αCD3scFv and αCD137scFv was detected in vector-transduced MMC cells using antibody staining (Fig. 2A) and expression of IL-15 and LIGHT by testing the culture supernatants from vector-transduced MMC cells by ELISA (Fig. 2B and C). In conclusion, all vectors efficiently expressed their immunoadjuvant in MMC cells. Next, the functionality of the expressed immunoadjuvants was assessed using standard immunoassays. Towards this goal, non-transduced and vector-transduced MMC cells were incubated with splenocytes of naïve syngeneic *neu*-tg mice at different effector:target (E:T) ratios. Activation (IFN-γ secretion; Fig. 2D) and proliferation (^{3}H-thymidine

incorporation; Fig. 2E) of splenocytes and the resulting cytotoxicity towards MMC cells (CPE; Fig. 2F, 2G) was tested. With the exception of Ad.αCD3, all other Ad-vectors only minimally increased the IFN-γ secretion and splenocyte proliferation when compared to Ad.zero or mock-infection (Fig. 2D and E) and this did not induce cytotoxicity towards MMC cells (Fig. 2F). In contrast, Ad.αCD3 mediated a strong increase of splenocyte activation (~8-fold increase of IFN-γ secretion; Fig. 2D), vigorous splenocyte proliferation (~10-fold increase of ^{3}H-incorporation; Fig. 2E) and importantly, splenocyte-mediated cell death in 100% of MMC cells (Fig. 2F and G). Notably, CD3-activation with an agonistic anti-CD3scFv bypasses T cell receptor activation and is routinely used for antigen-unspecific *in vitro* expansion of T cells. The observed lymphocyte activation and MMC cell killing by membrane-bound anti-CD3scFv in this assay was therefore most likely in an antigen-non-specific manner.
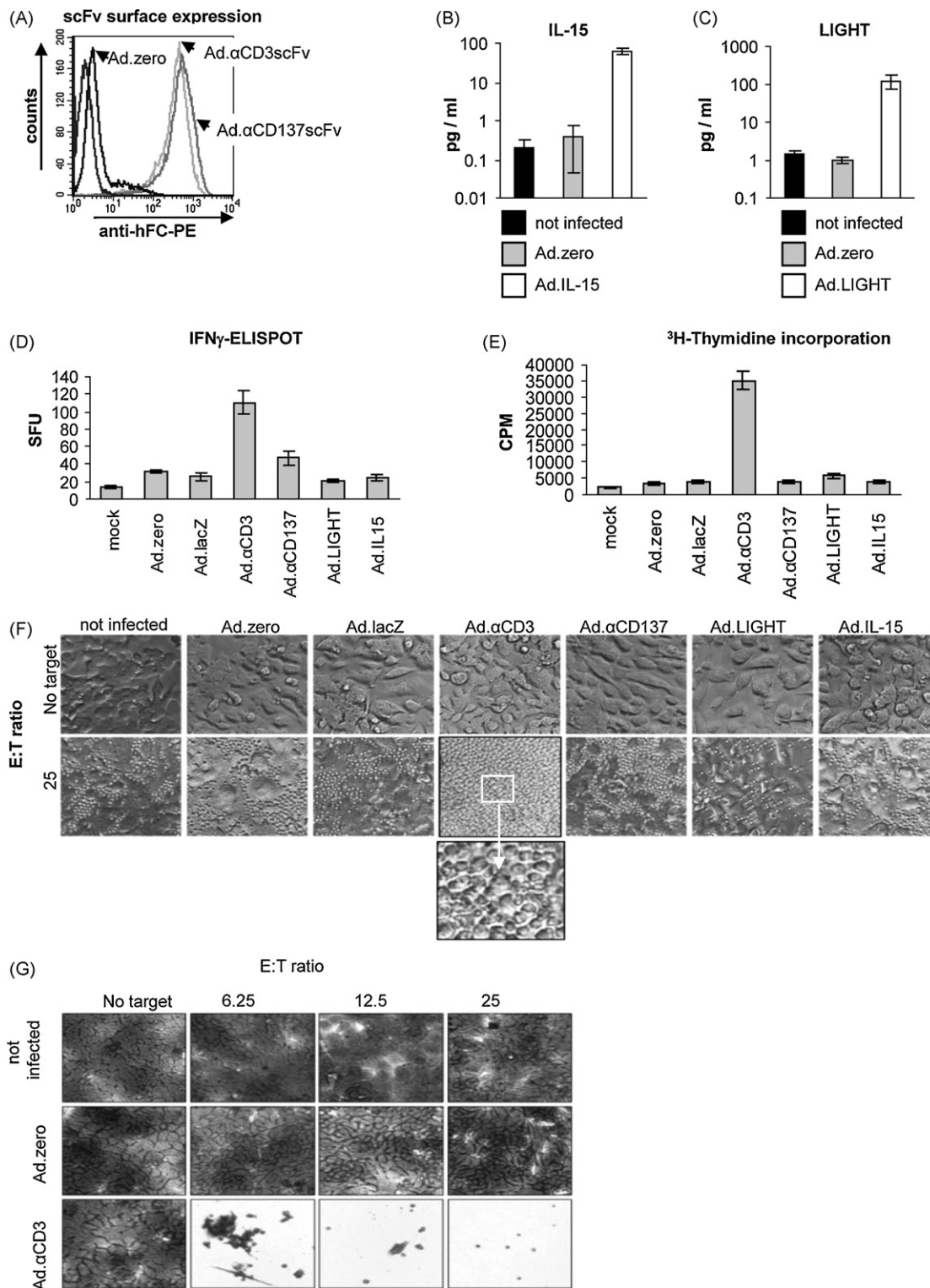
Fig. 2. Ad-mediated immunoadjuvant-expression *in vitro*. (A) Detection of membrane-bound αCD3scFv and αCD137scFv expression on MMC cells 48 h post infection (p.i.; MOI 100 pfu/cell) using anti-IgG-Fc-PE antibody and flow cytometry. (B and C) Quantification of IL-15 and LIGHT protein expression using ELISA assays with the supernatants of vector-transduced MMC cells (5 days p.i.; MOI 100 pfu/cell). (D and E) Quantification of activation (IFN-γ secretion) and proliferation ([3]HT incorporation) of splenocytes. MMC cells (cultured in T cell medium) were infected with Ad-vectors (MOI 100 pfu/cell). 24 h later fresh syngeneic splenocytes (from naïve *neu*-tg mice) were added (E:T ratio 100) and incubated for 2 days. Splenocytes were harvested and IFN-γ secretion was quantified via ELIspot assay. For the proliferation assay 1 μCi was added for 16 h and ^{3}H-thymidine incorporation was quantified using a scintillation counter. (F and G) Immunogenicity of MMC cells after Ad-vector transduction. MMC cells (cultured in T cell medium) were infected with Ad-vectors (MOI 50 pfu/cell). 24 h later fresh syngeneic splenocytes (from *neu*-tg mice) were added (E:T ratios are indicated) and incubated for 5 days. (F and G) Representative photographs of wells were taken (magnification 20×) before (F) and after (G) removal of splenocytes and crystal violet staining of MMC cells. Note that only Ad.αCD3 induced splenocyte-mediated MMC-cytotoxicity. (A, F and G) Representative flow chart overlays and pictures are shown; (B–E) Bars indicate the mean values and SD of experiments performed in duplicates; (F and G) These experiments were independently repeated with a similar outcome.

In summary, the data showed that syngeneic mouse MMC cells provide a novel model for testing human Ad5-based vectors. MMC cells supported Ad-vector infection and Ad-vector-mediated transgene expression. Furthermore, replication-competent Ad-vectors showed efficient expression of viral proteins, genomic replication and CPE induction in MMC cells, although *de-novo* production of infectious progeny viral particles was not supported. Finally, we identified several vectors that showed enhanced anti-tumor activity: Ad.IR-E1A/TRAIL and H101 were the most efficient vectors for replication-dependent MMC cell lysis, and Ad.αCD3 was the most efficient vector for triggering lymphocyte-mediated killing of MMC cells *in vitro*.

3.3. MMC tumors support Ad-vector transduction and replication in vivo

Our experiments showed that Ads are efficient tools for replication- or lymphocyte-mediated MMC cell killing *in vitro*. We hypothesized that Ad-transduction and anti-tumor efficacy might be affected (negatively or positively) due to various parameters that are different *in vivo*, e.g. presence of stroma cells, extracellular matrix, growth factors, cytokines, intratumoral hypoxia, 3-dimensional tumor architecture, tumor-infiltrating lymphocytes and/or cellular and non-cellular blood components that bind to Ads [3,4].

We therefore tested the functionality of Ad-vectors *in vivo*. Towards this goal, MMC cells were subcutaneously injected into syngeneic immunocompetent *neu*-tg mice, where they formed vascularized tumors that maintained an epithelial phenotype (E-cadherin surface expression) with cell clusters that were surrounded by extracellular matrix (laminin; Fig. S5). Various lymphoid cells infiltrated the MMC tumors, in particular CD4$^+$FoxP3$^+$ T cells (regulatory T cells), CD4$^+$FoxP3$^-$ (T helper cells), CD8$^+$ T cells and NK cells (Fig. S6).

To functionally evaluate Ads we injected them directly into MMC tumors. First, replication of Ad-vectors was tested. Replication-competent Ad.IR-E1A/TRAIL but not replication-deficient Ad.zero induced positive hexon staining 3 days after vector injection (Fig. 3A). This was in agreement with our *in vitro* data (Fig. 1). However, hexon staining was not detectable 7 days after vector injection (not shown). This indicated that vector replication is only present at early time points *in vivo*. We confirmed that MMC tumors supported Ad-vector replication using replication-dependent reporter gene expression with Ad.IR-based vectors that strictly express their reporter transgenes in a replication-dependent manner [10]. For Ad.IR-lacZ and Ad.IR-E1A/AP we again detected reporter gene expression 3 days post infection (Figs. 3B, S7) but not 7 days after injection (not shown). For Ad.IR-E1A/AP-injected tumors we found that positive AP staining co-localized with positive hexon staining, indicating co-expression of the reporter protein (AP) and viral protein (hexon) *in vivo* (Fig. S7). Finally, at day 7 post-injection no Ad-vector genomes, nor E1A mRNA expression were detectable in tumors by qPCR analyses. This indicates that Ad-transduced tumor cells are cleared by a CTL response within 7 days.

Having discovered that Ad-vector replication occurs at early time points (within less than 7 days post infection) in MMC tumors, we evaluated vectors that expressed their transgenes independently of viral replication. Overall, replication-independent expression was more efficient than replication-dependent transgene expression (compare lacZ expression via Ad.lacZ and Ad.IR-lacZ, Fig. 3B). This observation was in agreement with our *in vitro* data (compare Ad.GFP and Ad.IR-GFP; Fig. 1A). Next, immunoadjuvant-expressing vectors (Ad.αCD3/αCD137/IL-15/LIGHT) were tested. *In vivo* expression of the respective immunoadjuvant transgenes was confirmed using qRT-PCR 48 h post intratumoral vector injection (data not shown). In the case of IL-15 we did detect that this cytokine was already expressed inside the tumor prior to injection of the vector and that infection with Ad.IL-15, but not with Ad.zero, increased IL-15 transcript levels (~3.6-fold, Fig. S8).

Next, the transduction efficacy with replication-deficient Ad-vectors was evaluated more quantitatively using flow cytometry. For this purpose MMC tumors were injected with Ad.GFP. Tumors were harvested 24 h later and single-cell suspensions were generated and analyzed via flow cytometry for GFP reporter gene expression and E-cadherin as a surface marker for MMC cells. The *in vivo* transduction rate was ~32% of cells inside the tumor (Fig. 3C). Importantly, both MMC cells (E-cadherin high) and non-MMC cells (E-cadherin low) were transduced with equal efficacy inside the tumor (Fig. 3C). Using mean GFP fluorescence intensity as a quantitative marker for MMC cell transduction, the average multiplicity of infection (MOI) was determined as ~35 pfu/cell *in vivo* (Fig. S9). Finally, we assessed intratumoral apoptosis using TUNEL staining 5 days post infection (Fig. 3D). A replication-deficient Ad-vector (Ad.zero) was compared against a replication-competent Ad-vector (Ad.IR-E1A/TRAIL). Seven days after vector injection, significantly increased numbers of apoptotic cells were detectable in *both* Ad.zero and Ad.IR-E1A/TRAIL injected MMC tumors (these differences were less pronounced 3 days after injection; data not shown). This was surprising considering the fact that no vector replication was detectable at this time point. Apoptotic cells were also found in untreated tumors, indicating spontaneous apoptosis. The overall conclusion of the TUNEL staining was, however, limited since we found that only ~50% of the intratumoral cells were MMC cells (Fig. 3C) and the TUNEL assay did not indicate whether neoplastic or stroma cells were apoptotic *in vivo*.

Together the data showed that MMC tumors allowed for Ad-replication and Ad-mediated transgene expression in an immunocompetent setting *in vivo*, although Ad-replication was limited to less than 7 days post intratumoral injection.

3.4. In vivo efficacy of Ad-vectors against MMC tumors depends on T cells

To investigate the role of the immune system in the anti-tumor efficacy of Ad-vectors we established MMC tumors subcutaneously in syngeneic immunocompetent (*neu*-tg) and immunodeficient (SCID) mice. Similarly to *neu*-tg mice, SCID mice supported the formation of vascularized MMC tumors with similar intratumoral architecture (epithelial phenotype, extracellular matrix, nodule structure; Fig. S5). The median survival of MMC tumor-bearing mice was 14 days for both *neu*-tg and SCID mice, indicating that MMC tumors grow equally well in both mouse strains.

We first tested the anti-tumor efficacy of replication-competent vectors (H101, Ad.IR-E1A/TRAIL) compared to replication-deficient vectors (Ad.lacZ, Ad.zero; Fig. 4A). In SCID mice none of these vectors significantly increased median survival (MS) for more than 1.5 days. In contrast, all vectors significantly increased median survival in *neu*-tg mice for at least 5 days. These data strongly suggested that Ad-mediated anti-tumor efficacy was dependent on a functional immune system *in vivo* (compare SCID versus *neu*-tg mice; Fig. 4A). Additionally, together with the fact that MMC cells supported replication of these vectors *in vivo* (Figs. 3, S7), the data indicated that although Ad-replication increased anti-tumor efficiency *in vitro* (Figs. 1, S4), it was not an important component for anti-tumor activity *in vivo* (compare Ad.zero versus Ad.IR-E1A/TRAIL and H101; Fig. 1 versus Fig. 4A). The vector with the best anti-tumor efficacy in *neu*-tg mice was Ad.lacZ (median survival: 23 days, maximum survival: 32 days; Fig. 4A), which significantly increased survival compared to all other vectors (e.g. compare Ad.zero and Ad.lacZ; Fig. 4A). The fact that lacZ expression increased Ad-mediated anti-tumor efficacy only in *neu*-tg but not in SCID mice indicated that it
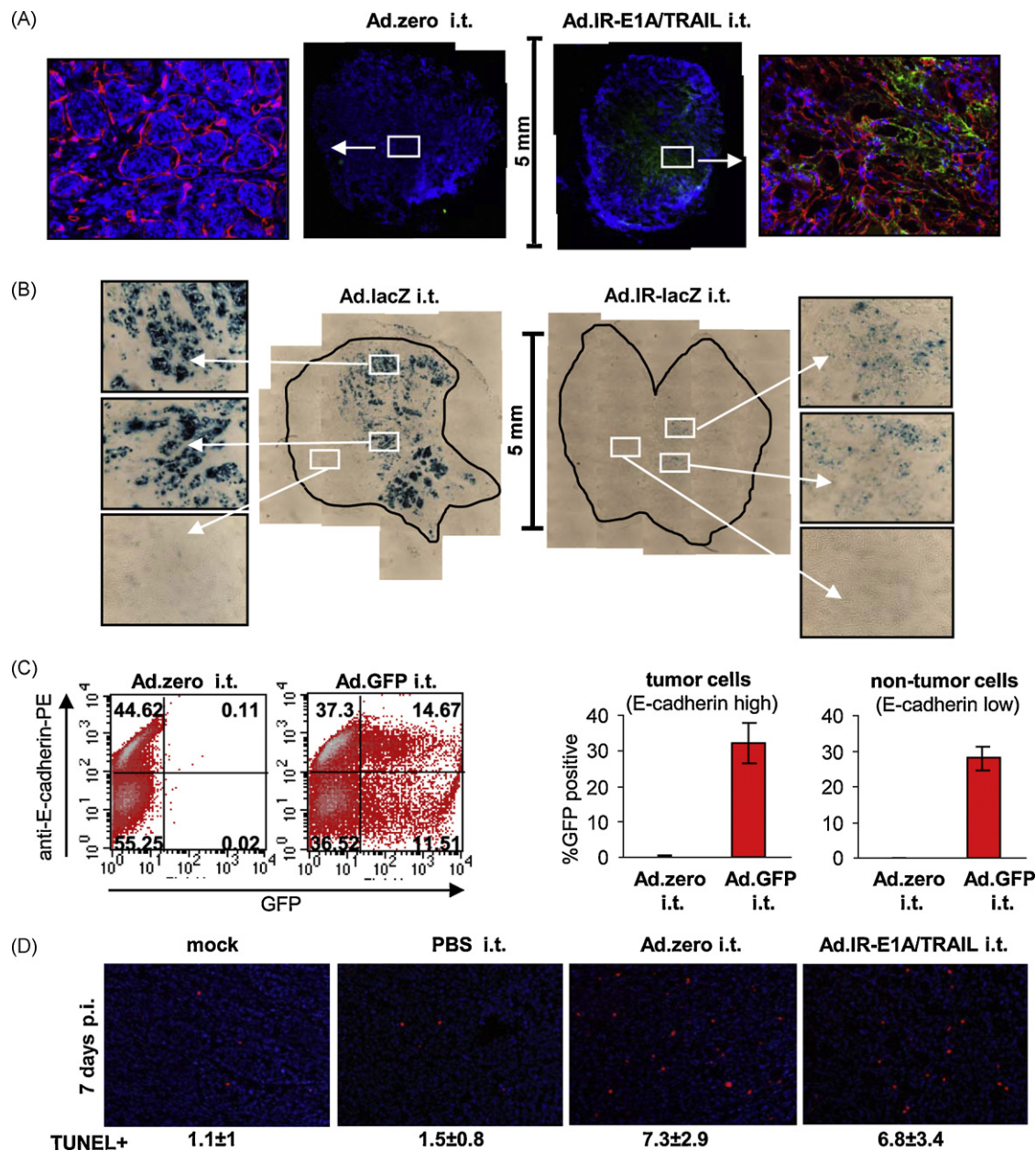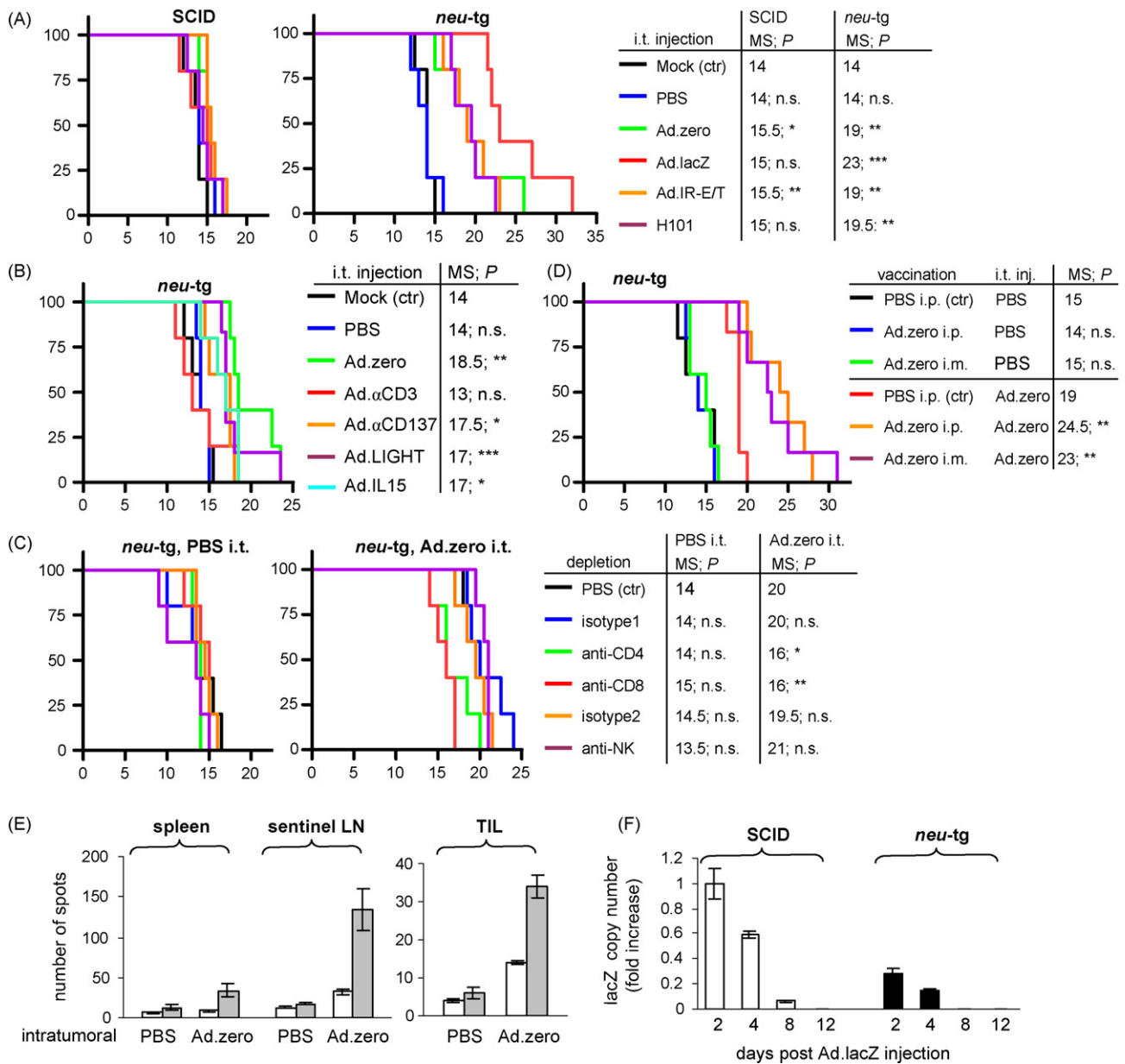
Fig. 3. Ad-vector function *in vivo*. For all experiments 5×10^5 MMC cells were injected subcutaneously into *neu*-tg mice and 1×10^9 pfu Ad-vector was injected once intratumorally when tumors reached a size of 3–4 mm diameter. (A) Hexon expression in MMC tumors 3 days after injection with Ad.zero or Ad.IR-E1A/TRAIL ($n = 3$ animals/group). Tumors were harvested, fixed, sectioned and stained for hexon (green), laminin (red) and nuclei (blue). Representative whole tumor sections (middle panels) and 20× magnifications (side panels) are shown. Laminin staining is only shown in the 20× magnifications. (B) LacZ expression in MMC tumors 3 days after injection with Ad.lacZ or Ad.IR-lacZ ($n = 3$ animals/group). Tumors were extracted, fixed, sectioned and stained for lacZ. Representative whole tumor sections (middle panels) and 20× magnifications (side panels) are shown. (C) GFP expression in MMC tumors 24 h after injection with Ad.zero or Ad.GFP ($n = 3$ animals/group). Tumors were collected, dispersed into single cells and analyzed for E-cadherin and GFP expression via flow cytometry. Percentages of GFP$^{-/+}$ MMC cells (E-cadherin high) and GFP$^{-/+}$ non-MMC cells (E-cadherin low) were determined. Left panel: Representative flow charts are shown. Right panel: Bars indicate mean and SD. (D) Detection of apoptotic cells in MMC tumors 5 days after intratumoral injection with Ad.zero or Ad.IR-E1A/TRAIL ($n = 3$ animals/group). Tumors were extracted, fixed, sectioned and stained for TUNEL positive cells (red) and nuclei (blue). Representative pictures are shown (magnification 20×). Mean number of TUNEL positive cells ± one SD is indicated. (For interpretation of the references to color in this figure legend, the reader is referred to the web version of the article.)

was also dependent on the immune system. Our findings were not expected from the previous *in vitro* data, which had indicated better efficacy for replication-competent H101 and Ad.IR-E1A/TRAIL than for replication-deficient Ad.zero and Ad.lacZ (Figs. 1, S4).

Since our data indicated that immunological mechanisms were responsible for the anti-tumor effect of Ad-vectors we next tested immunoadjuvant-expressing vectors *in vivo*. Ad.αCD3, Ad.αCD137, Ad.IL-15 and Ad.LIGHT were compared to Ad.zero in *neu*-tg mice (Fig. 4B). None of these immunoadjuvant-expressing vectors were

more anti-tumor efficient as compared to Ad.zero and Ad.αCD3 (which had shown the best immunostimulatory efficacy *in vitro*; Fig. 2D–G) surprisingly *decreased* significantly the immunotherapeutic potential of Ad-injection *in vivo*. Importantly, the "blank" (transgene-devoid) Ad-vector (Ad.zero) showed therapeutic effects that were dependent on a functional immune system. Based on these findings a series of subsequently experiments were performed exclusively using Ad.zero and Ad.lacZ in immunocompetent *neu*-tg mice.

Fig. 4. Ad-vector-mediated anti-tumor efficiency *in vivo*. For all experiments 5×10^5 MMC cells were injected subcutaneously into mice and 1×10^9 pfu Ad-vector was injected once intratumorally when tumors reached a size of 3–4 mm diameter. (A) Survival of SCID and *neu*-tg mice that were intratumorally injected with mock, PBS, Ad.zero, Ad.lacZ, Ad.IR-E1A/TRAIL or H101. (B) Survival of *neu*-tg mice that were intratumorally injected with mock, PBS, Ad.zero, Ad.αCD3, Ad.αCD137, Ad.IL-15 or Ad.LIGHT. (C) Survival of CD4+ T cell-, CD8+ T cell- and NK cell-depleted and non-depleted *neu*-tg mice that were intratumorally injected with PBS or Ad.zero. (D) Survival of Ad pre-immunized and non-immunized *neu*-tg mice that were intratumorally injected with PBS or Ad.zero. (E) ELIspot analysis for Ad-induced IFN-γ secretion. Spleens, sentinel lymph nodes (LN) and tumor-infiltrating lymphocytes (TIL) of *neu*-tg mice were harvested 10 days after intratumoral injection of Ad.zero or mock. For *in vitro* sensitization lymphocytes were pulsed with mock (white bars) or Ad.zero (gray bars). Bars indicate mean number of spots ± SD per 1×10^6 lymphocytes (spleen, LN; left panel) or 2.5×10^5 TIL (right panel). (F) LacZ transcript expression in Ad.lacZ intratumorally injected MMC tumors in SCID and *neu*-tg mice at different time points after injection quantified via real-time RT PCR. $y = 1$ for SCID tumors (day 2 p.i.). Bars indicate mean and SD. (A–D) $n = 5$ animals/group, except for Ad.LIGHT group: $n = 6$); (D) $n = 5$ animals/PBS i.t. group, $n = 7$ animals/Ad.zero i.t. group). (A–D) x-axis, days post tumor transplantation; y-axis, % survival; (E–H) $n = 3$ animals/group. MS, median survival; n.s., not significant; $P > 0.05$, $^*P < 0.05$, $^{**}P < 0.01$, $^{***}P < 0.001$ (logrank test).

To investigate which lymphoid cells were responsible for the Ad-vector-mediated anti-tumor effects we depleted CD4+ and CD8+ T cells and NK cells over the entire period of tumor growth and treatment. Efficacy of lymphocyte-depleting antibodies was confirmed via flow cytometry (Fig. S10). In short, depletion of CD8+ and CD4+ T cells but not depletion of NK cells inhibited the Ad-mediated anti-tumor efficacy, as indicated by significantly shorter median survival times (Fig. 4C). This indicated that CD4+ and CD8+ T cell-mediated immune responses were an essential component of Ad-mediated anti-tumor efficacy.

Most humans develop CD4+ and CD8+ T cell-dependent anti-Ad immunity early in life [11]. It was therefore next tested whether pre-existing adaptive immunity against Ads would interfere with T cell-mediated anti-tumor effects of Ad-vectors. For this purpose, naïve *neu*-tg mice were immunized via intramuscular or intraperitoneal Ad.zero injection (day 0, day 14) and tested for the titers of neutralizing anti-Ad antibodies (day 28). Both routes of immunization significantly increased titers of neutralizing anti-Ad antibodies (Fig. S11). We next established MMC tumors in naïve and Ad-immunized mice and injected Ad.zero (or PBS as a control)
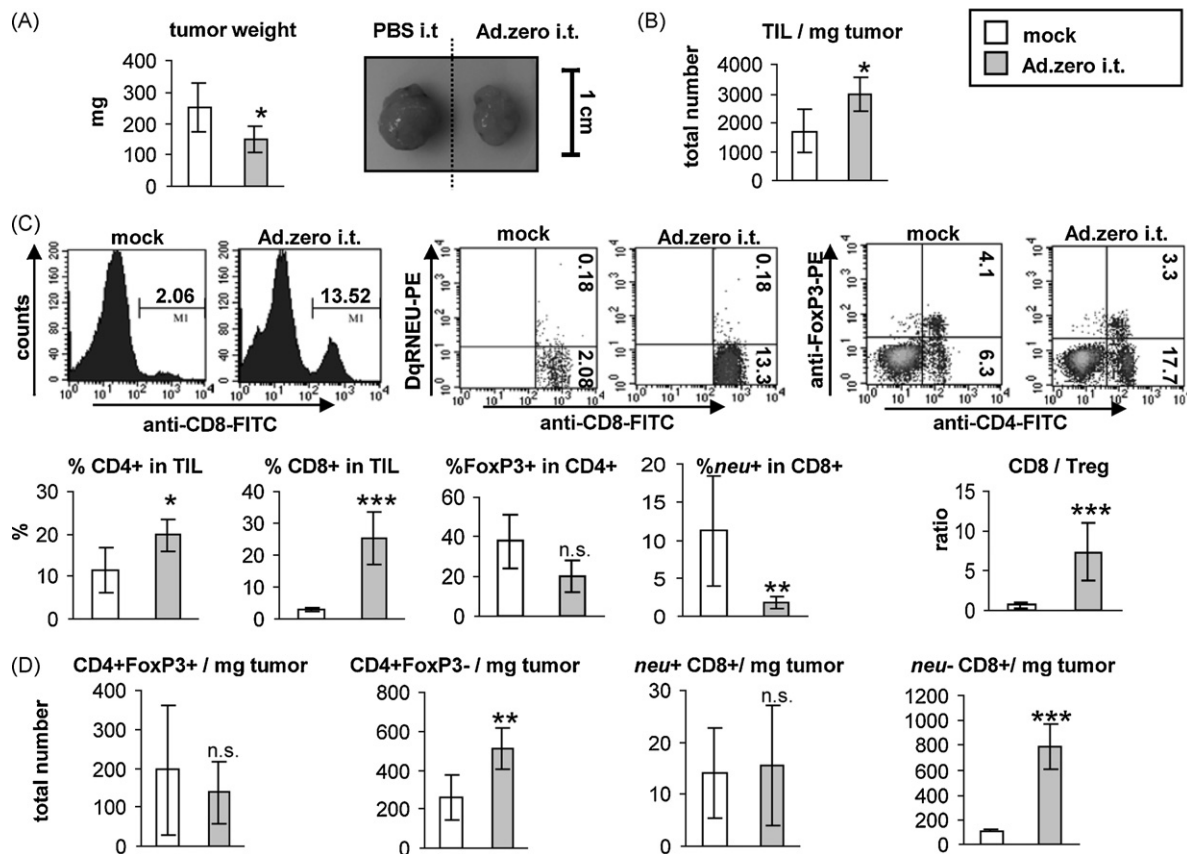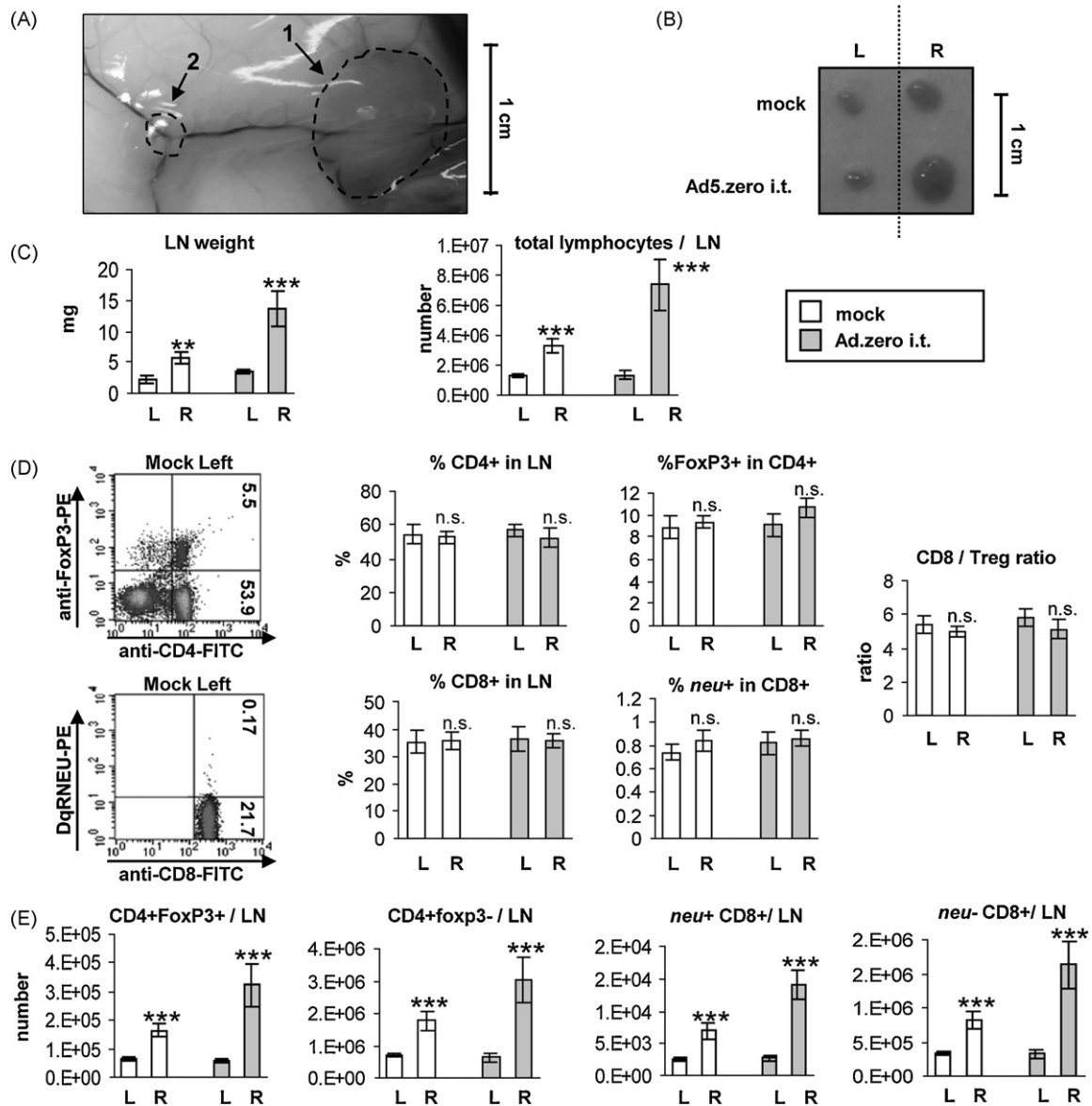
Fig. 5. Ad-induced T cell responses in the tumor microenvironment. 5×10^5 MMC cells were injected subcutaneously into *neu*-tg mice and 1×10^9 pfu Ad.zero or mock was injected once intratumorally when tumors reached a size of 3–4 mm diameter. Tumors were harvested 8 days after injection ($n = 5$ animals/group). (A) Left panel. Tumor weight. Right panel. Representative pictures of MMC tumors. (B) Total tumor-infiltrating lymphocytes (TIL) were extracted and counted and TIL/mg tumor calculated. (C) Upper panel. Percentages of $neu^{-/+}CD8^+$ T cells, regulatory T cells ($CD4^+FoxP3^+$) and T helper cells ($CD4^+FoxP3^-$) were determined using flow cytometry. Representative flow charts are shown. Lower panel: Percentages of $CD4^+$ and $CD8^+$ T cells in TIL, FoxP3 in $CD4^+$ and neu^+ in $CD8^+$ T cells are shown. Ratio of CD8/Treg was calculated. (D) Total amount of different lymphocyte populations per mg tumor was calculated using the data from B and C. (A–D) Bars indicate mean and SD. $P > 0.05$, n.s. (not significant); $^*P < 0.05$; $^{**}P < 0.01$; $^{***}P < 0.001$ (two-sided Student's t-test).

into the tumor (Fig. 4D). Surprisingly, we observed an *increased* anti-tumor efficacy of Ad.zero in Ad-immunized animals as indicated by significantly increased median survival times (Fig. 4D). Considering this result, we hypothesized that the Ad-specific T cell-mediated response could be a component of Ad-mediated anti-tumor efficacy. Therefore we assessed whether the frequency of T cells with Ad-antigen specificity would change in tumor infiltrating lymphocytes (TIL), sentinel lymph nodes or spleen 10 days after intratumoral Ad-injection. Importantly, we found that intratumoral Ad-injection significantly increased the number of Ad-reactive T cells in all tested lymphocyte compartments (Fig. 4E). The increase was ~2.4-fold for TIL, ~3.7-fold for splenocytes and ~4.2-fold for sentinel LN, respectively. This indicated that intratumoral Ad.zero injection triggered the expansion and/or infiltration of anti-Ad T cells inside both the lymphoid organs and the tumors. We hypothesized that one possible mechanism by which anti-Ad T cells could inhibit MMC tumor growth would be direct cell killing of Ad-transduced cells, considering that (a) CTLs are a natural component of the anti-adenoviral immune response during natural Ad-infection [11,15,16], (b) MMC cells can present antigens via major histocompatibility complex (MHC) class I and II [23,24], (c) Ad.zero showed Ad-hexon background expression in MMC cells (Fig. 1C), which is generally considered to favor MHC class I epitope presentation of viral proteins [34]. In order to test whether Ad-transduced MMC cells were preferentially eradicated by the immune system *in vivo* we next injected Ad.lacZ into MMC

tumors that were established in SCID (immunodeficient) or *neu*-tg (immunocompetent) mice. Tumors were harvested at different days post injection and lacZ transgene expression was quantified using real-time RT PCR (Fig. 4F). In both types of mice a continuous decrease of lacZ expression was detectable over time. However, lacZ expression was overall significantly decreased in *neu*-tg mice as compared to SCID mice. On day 2 and 4 post injection, intratumoral lacZ transcript levels were ~4-fold lower in *neu*-tg mice. Importantly, on day 8 post injection lacZ expression was detectable only in SCID mice but not in *neu*-tg mice. This result indicated that Ad.lacZ transduced MMC cells had a significantly shorter life span in immunocompetent mice compared to immunodeficient mice.

Overall, the data suggested that the anti-tumor efficacy of intratumoral Ad-injection was dependent on immune responses mediated by $CD4^+$ and $CD8^+$ T cell but not NK cells. Ad-specific T effector cells appeared to be an important component of this response, since (a) T effector cells with Ad-specificity expanded inside the tumor microenvironment and lymphoid organs (Fig. 4E), (b) Pre-existing anti-Ad immunity increased therapeutic efficacy of Ad-injection (Fig. 4D) and (c) Ad-transduction shortened the life span of transduced MMC cells in immunocompetent animals (Fig. 4F). Immunoadjuvant-expression and Ad-replication both failed to enhance anti-tumor efficacy *in vivo* (Fig. 4A and B), although these strategies had shown anti-tumor efficacy *in vitro* (Figs. 1 and 2). Notably, Ad-mediated lacZ reporter gene expression

Fig. 6. Ad-induced T cell responses in the tumor-draining lymph node. 5×10^5 MMC cells were injected subcutaneously into the right flank of *neu*-tg mice and 1×10^9 pfu Ad.zero or PBS was injected once intratumorally when tumors reached a size of 3–4 mm diameter. Inguinal tumor-draining (sentinel) lymph nodes (right-flank) and contra-lateral non-tumor-draining (non-sentinel) lymph nodes (left flank) and spleens (Fig. S12) were harvested 6 days after intratumoral injection (*n* = 5 animals/group). L = left flank; R = right flank. (A) Representative picture of sentinel LN and MMC tumor *in situ*. Note the vascularization of tumor and LN. (B) Representative picture of sentinel LN (R) and non-sentinel LN (L). (C) LN weight (left panel) and total lymphocyte number per LN (right panel). (D) Percentages of *neu*$^{-/+}$CD8$^+$ T cells, regulatory T cells (CD4$^+$FoxP3$^+$) and T helper cells (CD4$^+$FoxP3$^-$) were determined using flow cytometry. Left panel: Representative flow charts are shown. Middle panel: Percentages of CD4$^+$ and CD8$^+$ T cells in TIL, FoxP3$^+$ in CD4$^+$ and *neu*$^+$ in CD8$^+$ T cells are shown. Right panel: Ratio of CD8/Treg was calculated. (E) Total amount of different lymphocyte populations per LN was calculated using the data from (C and D). (C–E) Bars indicate mean and SD. $P > 0.05$, n.s. (not significant); $^*P < 0.05$; $^{**}P < 0.01$; $^{***}P < 0.001$ (two-sided Student's *t*-test).

increased immune-mediated therapeutic efficacy *in vivo* (Fig. 4A) but not *in vitro* (Figs. 2, S4).

3.5. In vivo T cell responses inside the tumors, tumor-draining lymph nodes and spleen from mice with Ad-transduced MMC tumors

Immune responses to antigens (e.g. adenoviral- or tumor-associated antigens) are generally generated in secondary lymphoid organs (lymph node or spleen) from which activated immune cells spread into the periphery (e.g. to other lymphoid organs, the infection- and/or tumor-sites). Lymphoid organs provide optimal conditions (in particular for antigen-presentation and co-stimulation via antigen presenting cell [APCs]) for T cell expansion.

We therefore tested the effect of intratumoral Ad-injection on (a) the tumor microenvironment (primary site of infection), (b) the tumor-draining (sentinel) lymph nodes and (c) the spleen. Spleen and LN were both investigated since antigens can either be transported with the blood stream or with the lymphatic system (passively or actively by migrating APCs). The following studies were focused exclusively on Ad.zero since this vector allowed us to determine the effect of the Ad-vector system itself.

3.5.1. Tumor microenvironment

First, immune responses in the microenvironment of Ad-infected tumors were investigated. We focused exclusively on CD4$^+$ and CD8$^+$ T cells, since our previous data showed that they were

essential and sufficient for Ad-mediated anti-tumor efficacy *in vivo* (Fig. 4C). In previous studies anti-Ad T cell responses peaked approximately one week post intravenous administration in mice [35]. We therefore harvested tumors 8 days post intratumoral Ad.zero (or mock) injection. Tumors were weighted, then tumor-infiltrating lymphocytes (TIL) extracted, counted, and analyzed via flow cytometry (Fig. 5).

3.5.2. T cell responses in untreated tumors

We determined the percentage of CD4$^+$ and CD8$^+$ T cells in TIL using flow cytometry (Fig. 5C). In order to specifically measure CD8$^+$ T cells that were reactive towards the immunodominant $neu_{420-429}$-epitope, the corresponding tetramer was used (see Fig. 5C and Section 2). In order to distinguish CD4$^+$ T helper from CD4$^+$ T regulatory cells (Tregs) intracellular staining for FoxP3 was used (Fig. 5C). FoxP3 is a sensitive and specific marker for Tregs, since FoxP3 expression is essential for the function of Tregs and not present in T helper cells [36]. Surprisingly, we found that the majority of T cells in the TIL of untreated tumors were CD4$^+$ T cells (~12% of TIL), whereas CD8$^+$ T cells were only a minor T cell fraction (~2% of TIL). Infiltration of T cells into the MMC tumor microenvironment was confirmed using immunohistochemistry (Fig. S6). Interestingly, ~38% of intratumoral CD4$^+$ T cells were FoxP3$^+$ (Fig. 5C), which was in stark contrast to other lymphocyte compartments. In particular, in the spleen (Fig. S12) and LN (Fig. 6D) only ~9% of CD4$^+$ T cells were FoxP3$^+$. Overall the ratio of CD8$^+$ T cells towards Tregs was lower in TIL (~0.7) as compared to LN (~5.5) or spleen (~4). This indicated a reversed effector/suppressor T cell ratio inside untreated MMC tumors (in particular an abundance of CD4$^+$FoxP3$^+$ Tregs over CD4$^+$ T helper cells and CTLs). Interestingly, ~12% of intratumoral CD8$^+$ T cells were specific for the immunodominant $neu_{420-429}$ epitope (Fig. 5C). This was again different from the peripheral lymphoid organs: in the spleen (Fig. S12) and LN (Fig. 6D) only ~0.3 and ~0.7% of CD8$^+$ T cells were specific for the $neu_{420-429}$ epitope (neu^+), respectively. Overall, the data indicated that untreated MMC tumors were selectively enriched for both regulatory T cells and neu^+ CD8$^+$ T cells. Surprisingly, the natural attraction of neu-specific CTLs into the tumor was apparently not sufficient to suppress tumor growth, which was also indicated by the fact that MMC cells formed tumors in immunocompetent neu-tg mice, CD8$^+$ T cell-depleted neu-tg mice and SCID mice with equal efficacy (Fig. 4A and C).

3.5.3. Ad-induced T cell responses

The tumor weight was significantly decreased in Ad.zero-injected tumors, whereas the total number of TIL/mg tumor was significantly increased as shown in Fig. 5A and B. Using flow cytometry we observed a strong increase of tumor-infiltrating CD8$^+$ T cells (from ~2% to ~24% of TIL; Fig. 5C). This significantly increased the CD8/Treg ratio from ~0.7 to ~7.4 (the latter ratio was comparable to lymphoid organs; see Figs. 6D, S12). However, the number of neu^+ CTLs did not increase in TIL (Fig. 5C). As a result, the percentage of neu-specificity in the CD8$^+$ T cell population actually decreased significantly (from ~12% to ~2%; Fig. 5D). This indicated that Ad-injection induced infiltration of CD8$^+$ T cells into the tumor microenvironment that were specific for antigens others than neu. Furthermore, we observed that Ad-injection led to an increase of CD4$^+$FoxP3$^-$ T cells inside the tumor whereas the number of intratumoral Tregs (CD4$^+$FoxP3$^+$) remained unchanged (Fig. 5D). This significantly decreased the percentage of FoxP3$^+$ cells in CD4$^+$ T cells from ~38% to ~20% and indicated that incoming CD4$^+$ T cells had an effector and not a suppressor phenotype (Fig. 5C). Corresponding to these data, quantification of IFN-γ and TGF-β expression at this time point also showed a ~167% increase for IFN-γ and ~19% decrease of TGF-β1 transcript levels, although these differences did not reach statistical significance (Fig. S13). IFN-γ is a hallmark

cytokine for CD4$^+$ Th1 cells, whereas TGF-β1 has been shown to mediate immunosuppressive functions of CD4$^+$FoxP3$^+$ Tregs [37].

3.5.4. Tumor-draining lymph nodes

We next investigated T cell responses inside the lymph nodes (Fig. 6) and spleen (Fig. S12). Spleen, sentinel LN (R, right flank) and non-sentinel LN (L, left flank) were harvested from animals 6 days post intratumoral Ad.zero (or mock) injection. Spleens and LN were weighted, lymphocytes extracted and total lymphocyte numbers per spleen/LN determined and flow-cytometry analysis was used to determine the percentage of different T cell populations.

3.5.5. T cell responses in untreated mice

MMC tumors naturally triggered an increase in LN weight and the number of lymphocytes in the sentinel LN but not in the non-sentinel LN or spleen (Figs. 6B and C, S12). According to flow-cytometry analysis the percentage of CD4$^+$FoxP3$^{-/+}$ and $neu^{-/+}$CD8$^+$ T cells was the same in the sentinel and non-sentinel LN (Fig. 6D). However, due to the increased total number of lymphocytes in the sentinel LN (Fig. 6C), both types of T cells increased there (Fig. 6E), i.e. MMC tumors triggered a T cell response in the sentinel LN that included the induction and expansion of both immunosuppressive (CD4$^+$FoxP3$^+$) and tumor-specific T effector cells (neu^+CD8$^+$ T cells). This was not observed inside the non-sentinel LN or spleen (Figs. 6E, S12).

3.5.6. Ad-induced T cell responses

The weight and cell number of the sentinel LN was further increased by intratumoral Ad-injection (Fig. 6B and C), while there was no change of the weight or cell number of the spleen or non-sentinel LN; Figs. 6B and C, S12). The percentage of CD4$^+$FoxP3$^{-/+}$ and $neu^{-/+}$CD8$^+$ T cells in the sentinel LN remained constant (Fig. 6D), but the total number of all T cell sub-populations increased (Fig. 6E). Therefore, we conclude that intratumoral Ad-injection had an immunoadjuvant effect on the induction of CD4$^+$FoxP3$^{-/+}$ and $neu^{-/+}$CD8$^+$ T cells inside the tumor-draining LN (Fig. 6B–E).

Overall, intratumoral Ad-injection induced T cell responses mainly in tumors and sentinel LN. In the tumor-draining LN both neu-specific (Fig. 6E) and Ad-specific T cells (Fig. 4E) increased significantly, indicating the simultaneous expansion there of T cell clones specific for both antigens. In contrast, in the tumors there was only an increase of T effector cells with Ad-specificity in response to *in situ* Ad vaccination (Figs. 4E, 5D).

4. Discussion

Immunosuppression in the tumor microenvironment, primarily mediated by regulatory T cells (Tregs), prevents the generation of an immune response to tumor-associated self-antigen(s). One way to circumvent this problem is to localize to the tumor a strong non-self-antigen to which there is no tolerance. In this study we establish a rationale for a T cell-mediated cancer immunotherapy based on the facts that adenoviruses have not evolved efficient mechanisms to establish immune tolerance and that the immune system has evolved to efficiently recognize Ads as strong immunogens and to trigger Ad-specific T cell responses that are not suppressed by peripheral tolerance mechanisms, in particular Tregs.

There is an emerging picture that the same mechanisms that prevent autoimmunity also inhibit anti-tumor immune responses. The central problem in cancer immunotherapy is that most tumor-associated antigens (e.g. neu) are non-mutated self-antigens that have triggered both central and peripheral tolerance. Central tolerance is established by selection in the thymus: T cells bearing T cell receptors (TCRs) with high affinity for self-antigen are eliminated through apoptosis [38]. Additionally, peripheral T cell tolerance is required to suppress the remaining auto-reactive T cells in the

periphery. Recent studies showed that, besides myeloid-derived suppressor cells and immature dendritic cells, a specialized subset of regulatory T cells (Tregs) is pivotal for maintaining peripheral immune tolerance [36]. Nevertheless, we and others have shown that *neu*-specific T effector cell immunity can be triggered spontaneously or vaccine-induced in ovarian and breast cancer patients, but this anti-tumor immunity has mostly failed to show clinical benefits [39,40]. There is accumulating evidence that multiple types of cancers, including ovarian and breast cancer, actively recruit and induce Tregs inside their microenvironment for the purpose of locally suppressing CTLs with tumor-antigen specificity [36,41,42].

MMC tumors in *neu*-tg mice spontaneously triggered *neu*-specific T effector cells inside the sentinel lymph nodes (Fig. 6), which poorly infiltrated tumors and were functionally inactive in the tumor microenvironment (Figs. 4 and 5) and these findings are consistent with the previous observation from patients with breast or ovarian cancer [39–42]. We have previously shown in *neu*-tg mice that depletion of regulatory T cells enabled activation and clonal expansion of *neu*-specific CD8⁺ T cells *in vivo*, which subsequently mediated MMC tumor regression [23]. Together with the findings of this study that MMC tumors selectively enriched *neu*-specific CD8⁺ *and* regulatory T cells inside the tumor microenvironment (Fig. 5) this indicated a central role of Tregs in mediating immune tolerance towards MMC cells in this model.

MMC cells/tumors supported Ad-transduction and Ad-replication *in vitro* (Figs. 1 and 2) and *in vivo* (Fig. 3). This, together with the possibility to quantify both anti-Ad and anti-*neu* responses, allowed us to analyze the role of the immune system in Ad-vector-mediated anti-tumor efficacy in a comprehensive manner. We showed that one injection of MMC tumors with Ad (1×10^9 pfu) resulted in the transduction of ~32% of cells inside the tumor microenvironment (Fig. 3C) with an average MOI of ~35 pfu/cell (Fig. S9). Replication of vectors was limited to less than 7 days in *neu*-tg mice (Fig. 3). Ad-transduction was also transient (less than 8 days) in *neu*-tg mice but significantly longer in SCID mice (Fig. 4F), which indicated an immune response towards Ad-transduced cells. We conclude that immune responses limited the efficacy of Ads as gene transfer vectors and Ad-vector injection would be required at least every 8 days to induce continuous expression of a transgene inside MMC tumors.

The main conclusion from our study is that *in situ* injection with replication-deficient, transgene-devoid Ad-particles was capable of inducing immune responses that inhibited tumor growth (Fig. 4). We show that the main effector-components of Ad-mediated anti-tumor efficacy were CD4⁺ and CD8⁺ T cells (Fig. 4C). The majority of Ad-triggered T effector cells were specific for Ad-antigens but not for the tumor-antigen *neu* and only T cells with Ad-specificity expanded inside the tumor microenvironment (Fig. 4E, Fig. 5D). Importantly, Ad-triggered T effector cells were functionally active despite the presence of intratumoral Treg-mediated immune tolerance that subdued *neu*-specific CTLs [23]. Ads were readily recognized as pathogens in *neu*-tg mice as indicated by induction of APC maturation (Fig. S14), (ii) Ad-specific T cells (Fig. 4E) and (iii) Ad-neutralizing antibodies (Fig. S11) upon Ad-administration. We conclude that Ad-derived antigens were "foreign" and apparently not protected by central or peripheral (Treg-mediated) immune tolerance in *neu*-tg mice and Treg depletion was therefore not required to enable the anti-Ad immune response. In contrast, tumor-associated antigen *neu* was a "self"-antigen and Treg-depletion has been shown to be required to enable an efficient anti-*neu* response in *neu*-tg mice [23]. The dominance of the adaptive anti-Ad immune response was not predicted by *in vitro* experiments (Fig. 2) and was only present *in vivo* (Figs. 4–6), most likely because clonal expansion of Ad-specific T cells was only supported in the *in vivo* setting. Importantly, Ad-mediated anti-tumor efficacy was further enhanced by pre-existing anti-Ad immunity (Fig. 4D).

We identified factors that enhanced, inhibited and did not influence the therapeutic efficacy of Ad-vectors *in vitro* and *in vivo*. Overall we observed that efficacy screenings of Ad-vectors *in vitro* or in SCID mice did not predict the mechanism or the anti-tumor efficacy of Ad-vectors in immunocompetent syngeneic mice.

4.1. Ad-replication

Replication-competent Ads (H101, Ad.IR-E1A/TRAIL) were more anti-tumor effective than E1/E3-deleted replication-deficient Ad.zero *in vitro* (Figs. 1, S4) but not *in vivo* (Fig. 4A). Ad-replication was only detectable at early time point (less than 7 days post injection; Fig. 3) and not an important effector mechanism *in vivo* (Fig. 4A). We speculate that the discrepancy between the *in vitro* and *in vivo* findings had multiple reasons: (a) *In vitro*, 100% of cells were transduced (Fig. 1), while *in vivo* the transduction rate was ~32% (Fig. 3C); (b) *de-novo* production of infectious viral particles was not supported by MMC cells *in vitro* (Fig. 1) and *in vivo* (Fig. 3); (c) Most importantly, Ad-replication was not required to induce anti-Ad responses *in vivo* (Fig. 4) and in agreement to this, other studies also previously found that innate and adaptive anti-Ad responses were independent of viral replication [12,43–45].

4.2. Pre-existing anti-Ad immunity

This is, to our knowledge, the first study to show that pre-existing immunity against Ads was a favorable factor for an effective anti-tumor response (Fig. 4D). A large majority of individuals in the human population develop adaptive anti-Ad immunity against wild-type Ad early in life [11]. Hence, we propose that a high proportion of the human population would be pre-conditioned for the proposed immunotherapy approach. Neutralizing antibodies (Fig. S10) did not interfere with Ad-mediated anti-tumor efficacy upon intratumoral Ad-application (Fig. 4D).

4.3. NK cells

NK cells were apparently not an effector component of Ad-vector-mediated anti-tumor activity (Fig. 4C). Expression of Ad E1 and E3 genes during natural Ad-infection has been proposed to render host cells susceptible to NK cell-mediated eradication [46]. However, the vectors used in this study were E1/E3-deleted and NK cell-inhibitory molecules (e.g. MHC complex I and II) were expressed on MMC cells [24], which both might have contributed to the fact that Ad-infected MMC cells were not susceptible to NK cells. Notably, H101 was only partly E1/E3-deleted and therefore NK cells might have played an active role in immune-mediated responses towards cells infected by this vector.

4.4. Immunoadjuvant expression

None of the tested immunoadjuvants (anti-CD3scFv, anti-CD137scFv, IL-15, LIGHT) enhanced the immunotherapeutic potential of Ads *in vivo* (Fig. 4B). This was surprising since especially anti-CD3scFv expression greatly enhanced the immunogenicity of MMC cells *in vitro* (Fig. 2). We speculate that the abundance of Tregs inside MMC tumors might have contributed to diminishing the therapeutic effect of anti-CD3scFv, since Tregs express CD3 and CD3-activation could potentially further enhance the immunosuppressive functions of these cells. The lack of co-stimulatory molecules (CD80 or CD86) on MMC tumors, which have been shown to be important for the anti-tumor activity of membrane-anchored anti-CD3 scFv, may have also contributed to poor therapeutic efficacy [28]. For anti-CD137scFv, we have previously shown that NK cells represent a main effector arm for immune-mediated anti-

tumor effects with this immunoadjuvants [29,30]. The fact that NK cells naturally did not have a major effector function against MMC cells (Fig. 4C) and that MMC cells naturally expressed NK cell inhibitors [24] might have contributed to the inefficacy of anti-CD137scFv in this model. Additionally, we have previously shown that, in particular in tumors that pre-dominantly utilize active immune-tolerance mechanisms, tumor-localized antibody-mediated immunotherapy (e.g. using anti-CD137scFv or anti-CTLA-4 antibody expression) was more effective when combined with interference of the function of immunosuppressive cells (e.g. using low-dose cyclophosphamide) [30,47].

4.5. LacZ reporter gene expression

LacZ unexpectedly increased the immunotherapeutic effect of Ads (Fig. 4A). We speculate that the increased *in vivo* effect of Ad.lacZ is due to the fact that lacZ (similarly to Ad-antigens) is not a self-antigen and therefore not protected by immune tolerance. LacZ is derived from *E. coli* and there are only minor amino-acid homologies to the corresponding murine and human enzymes (Fig. S15). Previous studies showed that the lacZ protein contained multiple epitopes that were presented via MHC class I and triggered lacZ-specific CTL responses [48,49]. We show in this study that this could be used to increase therapeutic immune response against cancer. Ad.lacZ also provided a proof-of-principle that expression of a transgene can be used to increase the immunotherapeutic potentials of Ads.

While MMC cells have the capability of antigen-presentation [23,24], many cancers lack this capability as a result of "immunoediting" [50]. In extensively "immunoedited" cancers other Ad-therapy components (in particular oncolysis, transgene-expression and/or NK cell responses) could therefore be dominant as compared to the T cell-mediated anti-Ad response. Furthermore, it has to be kept in mind that depletion of CD4+ or CD8+ T cell only partially inhibited the anti-tumor effects of Ad-injection (Fig. 4C). This indicated that other antigen-non-specific cellular (e.g. macrophages, killer dendritic cells) and non-cellular (e.g. growth-inhibiting or cytotoxic interleukins or cytokines) immune effector mechanisms might further contribute to Ad-mediated anti-tumor efficacy. Considering that >50% of intra-tumorally Ad-transduced cells were non-tumor cells (Fig. 3C) and that Ad-transduction significantly contributed to limiting the life span of all transduced cells (Fig. 4F), a significant proportion of the anti-tumor effect could be the result of immune-mediated killing or functional inhibition of stroma cells (e.g. endothelial cells and fibroblasts). Although further work is needed to understand by which immune mechanisms a tumor-localized Ad-vector inhibits tumor growth, we conclude that CD4+ or CD8+ T cells can be essential and that Ad-vector replication or transgene-expression are not always essential for Ad-mediated anti-tumor efficacy.

In the sentinel LN we found that intratumoral Ad-injection further enhanced the natural induction not only of Ad-specific but also of *neu*-specific T cells (Fig. 3D). Possible mechanisms for this phenomenon include that intratumoral Ad-injection increased expression of co-stimulatory molecules on APCs inside the sentinel LN (Fig. S14) and also increased intratumoral apoptosis as a potential source for tumor-antigen that can be processed and presented by APCs (Fig. 3D). It has been proposed that cross-presentation of tumor-antigens (derived from apoptotic tumor cells) is one main mechanism for the generation of tumor-specific T cell responses [51] and there has been another recent study that showed that viral infection (vesicular stomatitis virus) can synergize with the induction of tumor-specific immune responses inside the sentinel

LN [52]. Since MMC cells did not spontaneously spread from the primary tumor to form metastasis inside the LN (unpublished observation), we were not able to functionally evaluate the potential of this response to prevent micrometastasis into the draining lymph nodes.

We discovered and characterized a vaccination approach that localized Ad-vector to the tumor. This induced T effector responses that were anti-tumor efficient in the presence of intratumoral immunosuppression. Other analogous approaches that localize to the tumor certain surrogate antigens to which there is no central or peripheral tolerance might also prove successful.

Appendix A. Supplementary data

Supplementary data associated with this article can be found, in the online version, at doi:10.1016/j.vaccine.2009.03.074.

References

[1] http://wwwwileycouk/genetherapy/clinical/.
[2] Cattaneo R, Miest T, Shashkova EV, Barry MA. Reprogrammed viruses as cancer therapeutics: targeted, armed and shielded. Nat Rev Microbiol 2008;6(July (7)):529–40.
[3] Stone D, Liu Y, Shayakhmetov D, Li ZY, Ni S, Lieber A. Adenovirus–platelet interaction in blood causes virus sequestration to the reticuloendothelial system of the liver. J Virol 2007;81(May (9)):4866–71.
[4] Parker AL, Waddington SN, Nicol CG, Shayakhmetov DM, Buckley SM, Denby L, et al. Multiple vitamin K-dependent coagulation zymogens promote adenovirus-mediated gene delivery to hepatocytes. Blood 2006;108(Oct (8)):2554–61.
[5] Nemunaitis J, Khuri F, Ganly I, Arseneau J, Posner M, Vokes E, et al. Phase II trial of intratumoral administration of ONYX-015, a replication-selective adenovirus, in patients with refractory head and neck cancer. J Clin Oncol 2001;19(Jan (2)):289–98.
[6] Nemunaitis J, Ganly I, Khuri F, Arseneau J, Kuhn J, McCarty T, et al. Selective replication and oncolysis in p53 mutant tumors with ONYX-015, an E1B-55 kD gene-deleted adenovirus, in patients with advanced head and neck cancer: a phase II trial. Cancer Res 2000;60(Nov (22)):6359–66.
[7] Khuri FR, Nemunaitis J, Ganly I, Arseneau J, Tannock IF, Romel L, et al. A controlled trial of intratumoral ONYX-015, a selectively-replicating adenovirus, in combination with cisplatin and 5-fluorouracil in patients with recurrent head and neck cancer. Nat Med 2000;6(Aug (8)):879–85.
[8] Yu W, Fang H. Clinical trials with oncolytic adenovirus in China. Curr Cancer Drug Targets 2007;7(Mar (2)):141–8.
[9] Ni S, Ye X, Min L, Li Z-Y, Bernt K, Hu F, et al. Evaluation of different systems for tumor-specific gene expression from adenovirus vectors. Mol Ther 2002;5(5 (2)):S124.
[10] Steinwaerder DS, Carlson CA, Otto DL, Li ZY, Ni S, Lieber A. Tumor-specific gene expression in hepatic metastases by a replication-activated adenovirus vector. Nat Med 2001;7(Feb (2)):240–3.
[11] Lenaerts L, De Clercq E, Naesens L. Clinical features and treatment of adenovirus infections. Rev Med Virol 2008;18(Nov–Dec (6)):357–74.
[12] Muruve DA, Petrilli V, Zaiss AK, White LR, Clark SA, Ross PJ, et al. The inflammasome recognizes cytosolic microbial and host DNA and triggers an innate immune response. Nature 2008;452(March (7183)):103–7.
[13] Zhu J, Huang X, Yang Y. Innate immune response to adenoviral vectors is mediated by both Toll-like receptor-dependent and -independent pathways. J Virol 2007;81(Apr (7)):3170–80.
[14] Appledorn DM, Patial S, McBride A, Godbehere S, Van Rooijen N, Parameswaran N, et al. Adenovirus vector-induced innate inflammatory mediators, MAPK signaling, as well as adaptive immune responses are dependent upon both TLR2 and TLR9 in vivo. J Immunol 2008;181(Aug (3)):2134–44.
[15] Heemskerk B, van Vreeswijk T, Veltrop-Duits LA, Sombroek CC, Franken K, Verhoosel RM, et al. Adenovirus-specific CD4+ T cell clones recognizing endogenous antigen inhibit viral replication in vitro through cognate interaction. J Immunol 2006;177(Dec (12)):8851–9.

[16] Leen AM, Christin A, Khalil M, Weiss H, Gee AP, Brenner MK, et al. Identification of hexon-specific CD4 and CD8 T-cell epitopes for vaccine and immunotherapy. J Virol 2008;82(Jan (1)):546–54.

[17] Harrop R, Carroll MW. Viral vectors for cancer immunotherapy. Front Biosci 2006;11:804–17.

[18] Prestwich RJ, Harrington KJ, Pandha HS, Vile RG, Melcher AA, Errington F. Oncolytic viruses: a novel form of immunotherapy. Expert Rev Anticancer Ther 2008;8(Oct (10)):1581–8.

[19] Ternovoi VV, Le LP, Belousova N, Smith BF, Siegal GP, Curiel DT. Productive replication of human adenovirus type 5 in canine cells. J Virol 2005;79(Jan (2)):1308–11.

[20] Toth K, Spencer JF, Tollefson AE, Kuppuswamy M, Doronin K, Lichtenstein DL, et al. Cotton rat tumor model for the evaluation of oncolytic adenoviruses. Hum Gene Ther 2005;16(Jan (1)):139–46.

[21] Thomas MA, Spencer JF, La Regina MC, Dhar D, Tollefson AE, Toth K, et al. Syrian hamster as a permissive immunocompetent animal model for the study of oncolytic adenovirus vectors. Cancer Res 2006;66(Feb (3)): 1270–6.

[22] Bernt KM, Ni S, Tieu AT, Lieber A. Assessment of a combined, adenovirus-mediated oncolytic and immunostimulatory tumor therapy. Cancer Res 2005;65(May (10)):4343–52.

[23] Knutson KL, Dang Y, Lu H, Lukas J, Almand B, Gad E, et al. IL-2 immuno-toxin therapy modulates tumor-associated regulatory T cells and leads to lasting immune-mediated rejection of breast cancers in neu-transgenic mice. J Immunol 2006;177(July (1)):84–91.

[24] Knutson KL, Lu H, Stone B, Reiman JM, Behrens MD, Prosperi CM, et al. Immunoediting of cancers may lead to epithelial to mesenchymal transition. J Immunol 2006;177(Aug (3)):1526–33.

[25] Shayakhmetov DM, Papayannopoulou T, Stamatoyannopoulos G, Lieber A. Efficient gene transfer into human CD34(+) cells by a retargeted adenovirus vector. J Virol 2000;74(Mar (6)):2567–83.

[26] DiPaolo N, Ni S, Gaggar A, Strauss R, Tuve S, Li ZY, et al. Evaluation of adenovirus vectors containing serotype 35 fibers for vaccination. Mol Ther 2006;13(Apr (4)):756–65.

[27] Liao KW, Lo YC, Roffler SR. Activation of lymphocytes by anti-CD3 single-chain antibody dimers expressed on the plasma membrane of tumor cells. Gene Ther 2000;7(Feb (4)):339–47.

[28] Liao KW, Chen BM, Liu TB, Tzou SC, Lin YM, Lin KF, et al. Stable expression of chimeric anti-CD3 receptors on mammalian cells for stimulation of antitumor immunity. Cancer Gene Ther 2003;10(Oct (10)):779–90.

[29] Ye Z, Hellstrom I, Hayden-Ledbetter M, Dahlin A, Ledbetter JA, Hellstrom KE. Gene therapy for cancer using single-chain Fv fragments specific for 4-1BB. Nat Med 2002;8(Apr (4)):343–8.

[30] Yang Y, Yang S, Ye Z, Jaffar J, Zhou Y, Cutter E, et al. Tumor cells expressing anti-CD137 scFv induce a tumor-destructive environment. Cancer Res 2007;67(Mar (5)):2339–44.

[31] Waldmann TA. The biology of interleukin-2 and interleukin-15: implications for cancer therapy and vaccine design. Nat Rev Immunol 2006;6(Aug (8)):595–601.

[32] Yu P, Lee Y, Liu W, Chin RK, Wang J, Wang Y, et al. Priming of naive T cells inside tumors leads to eradication of established tumors. Nat Immunol 2004;5(Feb (2)):141–9.

[33] Sova P, Ren XW, Ni S, Bernt KM, Mi J, Kiviat N, et al. A tumor-targeted and conditionally replicating oncolytic adenovirus vector expressing TRAIL for treatment of liver metastases. Mol Ther 2004;9(Apr (4)):496–509.

[34] Heath WR, Carbone FR. Cross-presentation in viral immunity and self-tolerance. Nat Rev Immunol 2001;1(Nov (2)):126–34.

[35] Chen J, Hsu HC, Zajac AJ, Wu Q, Yang P, Xu X, et al. In vivo analysis of adenovirus-specific cytotoxic T lymphocyte response in mice deficient in CD28, fas ligand, and perforin. Hum Gene Ther 2006;17(June (6)):669–82.

[36] Yamaguchi T, Sakaguchi S. Regulatory T cells in immune surveillance and treatment of cancer. Semin Cancer Biol 2006;16(Apr (2)):115–23.

[37] Amstutz B, Gastaldelli M, Kalin S, Imelli N, Boucke K, Wandeler E, et al. Subversion of CtBP1-controlled macropinocytosis by human adenovirus serotype 3. EMBO J 2008;27(Apr (7)):956–69.

[38] Li MO, Flavell RA. TGF-beta: a master of all T cell trades. Cell 2008;134(Aug (3)):392–404.

[39] Disis ML, Knutson KL, Schiffman K, Rinn K, McNeel DG. Pre-existent immunity to the HER-2/neu oncogenic protein in patients with HER-2/neu overexpressing breast and ovarian cancer. Breast Cancer Res Treat 2000;62(Aug (3)):245–52.

[40] Knutson KL, Schiffman K, Disis ML. Immunization with a HER-2/neu helper peptide vaccine generates HER-2/neu CD8 T-cell immunity in cancer patients. J Clin Invest 2001;107(Feb (4)):477–84.

[41] Curiel TJ, Coukos G, Zou L, Alvarez X, Cheng P, Mottram P, et al. Specific recruitment of regulatory T cells in ovarian carcinoma fosters immune privilege and predicts reduced survival. Nat Med 2004;10(Sep (9)):942–9.

[42] Liyanage UK, Moore TT, Joo HG, Tanaka Y, Herrmann V, Doherty G, et al. Prevalence of regulatory T cells is increased in peripheral blood and tumor microenvironment of patients with pancreas or breast adenocarcinoma. J Immunol 2002;169(Sep (5)):2756–61.

[43] Kafri T, Morgan D, Krahl T, Sarvetnick N, Sherman L, Verma I. Cellular immune response to adenoviral vector infected cells does not require de novo viral gene expression: implications for gene therapy. Proc Natl Acad Sci U S A 1998;95(Sep (19)):11377–82.

[44] Muruve DA, Cotter MJ, Zaiss AK, White LR, Liu Q, Chan T, et al. Helper-dependent adenovirus vectors elicit intact innate but attenuated adaptive host immune responses in vivo. J Virol 2004;78(June (11)):5966–72.

[45] Yang Y, Nunes FA, Berencsi K, Furth EE, Gonczol E, Wilson JM. Cellular immunity to viral antigens limits E1-deleted adenoviruses for gene therapy. Proc Natl Acad Sci U S A 1994;91(May (10)):4407–11.

[46] McSharry BP, Burgert HG, Owen DP, Stanton RJ, Prod'homme V, Sester M, et al. Adenovirus E3/19K promotes evasion of NK cell recognition by intracellular sequestration of the NKG2D ligands major histocompatibility complex class I chain-related proteins A and B. J Virol 2008;82(May (9)):4585–94.

[47] Tuve S, Chen BM, Liu Y, Cheng TL, Toure P, Sow PS, et al. Combination of tumor site-located CTL-associated antigen-4 blockade and systemic regulatory T-cell depletion induces tumor-destructive immune responses. Cancer Res 2007;67(June (12)):5929–39.

[48] Yang S, Hodge JW, Grosenbach DW, Schlom J. Vaccines with enhanced costimulation maintain high avidity memory CTL. J Immunol 2005;175(Sep (6)):3715–23.

[49] Jooss K, Yang Y, Fisher KJ, Wilson JM. Transduction of dendritic cells by DNA viral vectors directs the immune response to transgene products in muscle fibers. J Virol 1998;72(May (5)):4212–23.

[50] Dunn GP, Bruce AT, Ikeda H, Old LJ, Schreiber RD. Cancer immunoediting: from immunosurveillance to tumor escape. Nat Immunol 2002;3(Nov (11)):991–8.

[51] Nowak AK, Lake RA, Marzo AL, Scott B, Heath WR, Collins EJ, et al. Induction of tumor cell apoptosis in vivo increases tumor antigen cross-presentation, cross-priming rather than cross-tolerizing host tumor-specific CD8 T cells. J Immunol 2003;170(May (10)):4905–13.

[52] Qiao J, Kottke T, Willmon C, Galivo F, Wongthida P, Diaz RM, et al. Purging metastases in lymphoid organs using a combination of antigen-nonspecific adoptive T cell therapy, oncolytic virotherapy and immunotherapy. Nat Med 2008;14(Jan (1)):37–44.